NTNU
Det skapende universitet

Måling av reaksjonsvarme og gass-/væskelikevekt for CO2 fangst i solventer med to væskefaser

Åsne Daling Nannestad

Industriell kjemi og bioteknologi
Innlevert: januar 2016
Hovedveileder: Hanna Knuutila, IKP

Norges teknisk-naturvitenskapelige universitet
Institutt for kjemisk prosessteknologi

Preface

This report is the final delivery of a master's thesis at the Norwegian University of Science and Technology (NTNU) at the Department of Chemical Process Technology (IKP). The report corresponds to 20 weeks of work and 30 study points in the period 25th.August 2015-17th.January 2016. Carbon Capture and Storage (CCS) is one of the mitigation strategies to globally reduce CO_2-emissions. This work studies the performance of new solvents for use in chemical absorption technology. I have always been concerned with environmental issues, and I find great motivation in working with a topic related to CCS. I do hope for CCS to become one of the future focus areas in global industry, with continued research and development of the technology.

I would like to thank my supervisor Associate Professor Hanna Knuutila at NTNU for helpful guidance, great suggestions and interesting discussions along the way. Her supervision has to a great extent contributed to increase my understanding of the topic and see new aspects of the results in this work. Inna Kim at SINTEF has been very helpful with training and issues related to the laboratory apparatus. I want to thank Ida Bernhardsen for helping me with ordering of chemicals and for interesting discussions. The weekly meetings with the small CO_2-group at the department has also contributed greatly to my motivation.

There has been long days in the laboratory and moments of frustration during the past months. However, I look back and see the 20 most educational weeks I have had at NTNU. I appreciate the opportunity I have had to focus on interesting subjects within the main scope, liberty to work independently and the possibilities to discuss my work with such academically strong personalities.

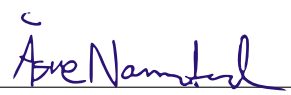

Åsne Daling Nannestad
Trondheim 16th.January 2016

Abstract

Absorption of CO_2 by amines is a well developed technology for CO_2-capture. However, there are several issues related to the current technology, such as high energy consumption, degradation of amines and kinetics. Research is constantly performed to come up with new and better alternatives of solvents to enhance the overall CO_2-capture performance.

Two novel solvents for CO_2 absorption are studied in this work. These are the tertiary amine 2-(diethylamino)-ethanol (DEEA) and the diamine 3-(methylamino)-propylamine (MAPA), with one primary and one secondary amine group. Different blends of the two amines has been experimentally tested. Heat of reaction for absorption of CO_2 into blends of DEEA and MAPA has been measured in a reaction calorimeter at the temperatures 40°C, 80°C and 120°C. A total of six blends have been studied, where each blend is tested twice at each temperature.

Three of the systems formed two liquid phases upon absorption of CO_2, whereas the three other remained as one phase. Generally, values for heat of absorption in the same solution at loadings up to around 0.3 are lower for T=40°C and highest at T=120°C. The heat of absorption steadily decreases for blends of DEEA-MAPA with increasing loading, unlike pure MAPA-water and DEEA-water systems, which have almost constant values up to a loading around 0.8.

Heat of reaction was also measured for absorption of CO_2 in Monoethanolamine (MEA)-water. MEA-water is a well studied system, and data obtained in this work were used fro validation. Results from this work correlates well with literature data at T=40°C and T=80°C. The results at T=120°C deviated slightly more, but within an acceptable range. Parallel experiments show relatively good agreement, indicating good reproducibility of data. VLE-data has also been calculated based on the changes in total pressure in the reactor at equilibrium between loadings. VLE-data in this work show generally good agreement with literature-data. The loadings of phase-transition were determined and were compared to the data for heat of absorption and VLE to see if the two-phase formation affects the values. No significant changes were observed, and any effect of two-phase formation is not proved.

One blend stands out as the better absorption solution. The blend of 3M DEEA+1.5M MAPA has the lowest values values for heat of absorption at high temperature, as well as high CO_2 partial pressure. Thus is desirable for desorption.

Sammendrag

Absorpsjon av CO_2 ved bruk av aminer er en velutviklet teknologi for CO_2-fangst. Likevel er det stort forbedringspotensial ved dagens teknologi, relatert til blant annet høyt energiforbruk, degradering av aminer og reaksjonshastighet. Det forskes kontinuerlig for å finne solventer som vil forbedre CO_2-fangstprosessen. Denne oppgaven tar for seg to nye solventer for CO_2 absorpsjon: Den tertiære aminen 2-(diethylamino)-ethanol (DEEA) og diaminen 3-(methylamino) -propylamine (MAPA), som har én primær- og én sekundær amingruppe. Ulike blandingsforhold av de to aminene er testet eksperimentelt. Det er målt absorpsjonsvarme for CO_2-absorpsjon i DEEA-MAPA- blandinger i et reaksjonskalorimeter ved temperaturene 40°C, 80°C og 120°C . Totalt seks ulike blandinger er testet, der hvert forsøk er utført to ganger ved hver temperatur.

Tre av blandingene dannet to væskefaser når en gitt mengde CO_2 var absorbert (loading), mens tre blandinger forble én væskefase gjennom hele forsøket. Generelt er verdiene for absorpsjonsvarme i samme løsning økende for økende temperatur opp til en loading rundt 0.3. I DEEA-MAPA-blandinger er absorpsjonsvarmen jevnt avtakende for økende loading. Dette er ulikt trenden i rene DEEA-vann- og MAPA-vannløsninger, som holder konstante absorpsjonsverdier opp til en loading rundt 0.8.

Tilsvarende absorpsjonsmålinger er utført for absorpsjon av CO_2 i Monoethanolamine(MEA)-vann. MEA-vann er et system det er gjort mye forskning på, og tidligere data fra andre forskere er brukt for å validere de resultater som er oppnådd i dette arbeidet. Resulatene stemmer godt overens for forsøk utført ved T=40°C og 80°C. Resulatene ved T=120°C avviker noe mer, men innen akseptable grenser. Parallelle forsøk viser stort sett like verdier, og indikerer god reproduserbarhet.

Gass-væske-likevekt(VLE)-data er beregnet basert på endringer i totaltrykk i reaktoren, ved likevekt mellom hver tilførsel av CO_2. VLE-data fra dette forsøket stemmer bra med litteraturdata. Det er også utført et sett av enkle eksperimenter for bestemmelse av loading der faseendringer skjer. Disse loadingene er sammenlignet med data for absorpsjonsvarme og VLE for å undersøke effekten av faseendring. Ingen betydelige endringer ble observert, og en slik effekt er ikke påvist.

Én blanding skiller seg ut som det beste alternativet som solvent i en absorpsjonsprosess. Blandingen med 3M DEEA+1.5M MAPA har de laveste verdiene for absorpsjonsvarme ved høy temperatur, og samtidig det høyeste partialtrykket, som er ønskelige egenskaper i desorpsjon av CO_2.

List of abbreviations

Abbreviation	Full name
GHG	Green House Gas
CCS	Carbon Capture and Storage
DI-water	De-ionized water
VLE	Vapour-Liquid-Equilibrium
MSDS	Material Safety Data Sheet
e-NRTL	electrolyte Non-Random Two-Liquid

List of symbols

Symbol	Description	Unit
H_i	Enthalpy of component i	J
α	Loading	$\frac{mol_{CO_2}}{mol_{amine}}$
Q	Cyclic Capacity	$\frac{molCO_2}{L_{solution}}$
R	Organic functional group	
Cp	Heat Capacity	$\frac{J}{mol}$
T_j	Temperature at point j	°C
q	Heat	J
$\frac{dM}{dt}$	Mass flow	$\frac{kg}{s}$
$FlowCP$	Product of mass flow and heat capacity in jacket fluid	$\frac{J}{s}$
C_{amine}	Concentration of amines	$\frac{mol_{amine}}{L}$
n_i	Number of moles of component i	mol
V	Volume	L
m	Mass	kg
p	Pressure	Pa
R	Gas constant	$\frac{J}{°Cmol}$
V_m	Molar volume	$\frac{L}{mol}$
ω	Acentric factor	
p_i	Partial pressure of component i	Pa
P	Total pressure	Pa

Contents

Chapter 1

Introduction

1.1 Background

The atmospheric concentration of greenhouse gases (GHG's) has increased significantly since the beginning of the industrial revolution in the early 17th century. The UN Climate report from 2014 (IPCC 2014) states that the global average temperature has increased in the same period, and will continue to increase as a consequence of higher GHG-concentration in the atmosphere. The phenomenon is referred to as *global warming*. According to the report, some of the consequences from higher average temperatures are lower food production, more extreme weather, pollution of the oceans, loss of species, raise of the sea level and less freshwater. The UN Climate Report states that global warming is, by 95 % probability, caused by anthropogenic GHG-emissons. The only positive thing about humans being responsible for climate changes is that we have the opportunity to counteract further changes. Scientists have estimated a rise in temperature of 2°C relative pre-industrial levels as the treshold of a sustainable future. If the GHG-emissions continue as today the temperature is predicted to rise by 4.6°C by the year 2100. Thus emissions need to be reduced, and several mitigation strategies are already available.

According to the UN climate report summary for policymakers (Edenhofer et al., 2014) Carbon Dioxide (CO_2) alone stands for 77% of the GHG-emissions, measured in tons of CO_2-equivalents. The main sources of emissions are burning of fossil fuels and deforestration. One of the mitigation strategies is Carbon Dioxide Capture and Storage (CCS). The aim of a CCS-process is to capture the CO_2 produced in combustion processes before it is

emitted to the atmosphere. Purified CO_2 is then compressed and transported to reservoirs for long-time storage. The cost of CCS is mainly related to the separation and compression part of the process, while transportation and storage are minor contributors to the overall energy consumption (Figueroa et al., 2008b). This report studies one aspect of the CCS-process, more specifically CO_2 capture by absorption.

1.2 CO_2-capture

'CO_2-capture' is in a sense the same as 'CO_2-separation'. The aim in CO_2-capture is to separate CO_2 from an inlet gas mixture, to obtain a high-purity CO_2-gas and an output gas mixture lean on CO_2. With present CO_2 capture technologies, capture is most efficiently performed on flue gas from larger point emission sources such as fossil- or biofuel power plants, or chemical industrial plants. It is estimated that a modern conventional power plant can reduce its emissions of CO_2 by 80-90% compared to a plant without capture (Yu et al., 2008). In 2013 it was estimated that more than 80% of the world's energy came from fossil fuel (IEA, 2013), which implies there is a fairly large potential in power plant CO_2 capture to reduce CO_2 emissions globally.

The capture process from fossil fuel/biofuel power plants and industry can be performed by three different routes; pre-combustion, post-combustion and oxyfuel-combustion. The routes are illustrated in Figure 1.1.

1.2.1 Pre-Combustion

In pre-combustion CO_2-capture a solid fuel is gasified, yielding a gas mixture of mainly CO_2, carbon monoxide (CO) and hydrogen (H_2), together with some hydrocarbons and small concentrations of other compounds. The gasification is followed by a water gas shift reaction where water, injected as steam, reacts with CO and produces CO_2 and H_2. CO_2 is separated from this gas mixture, yielding a purified CO_2-gas which can be sent to compression and storage, and an energy-intensive hydrogen-gasmixture which can be used for energy production (Kanniche et al., 2010).

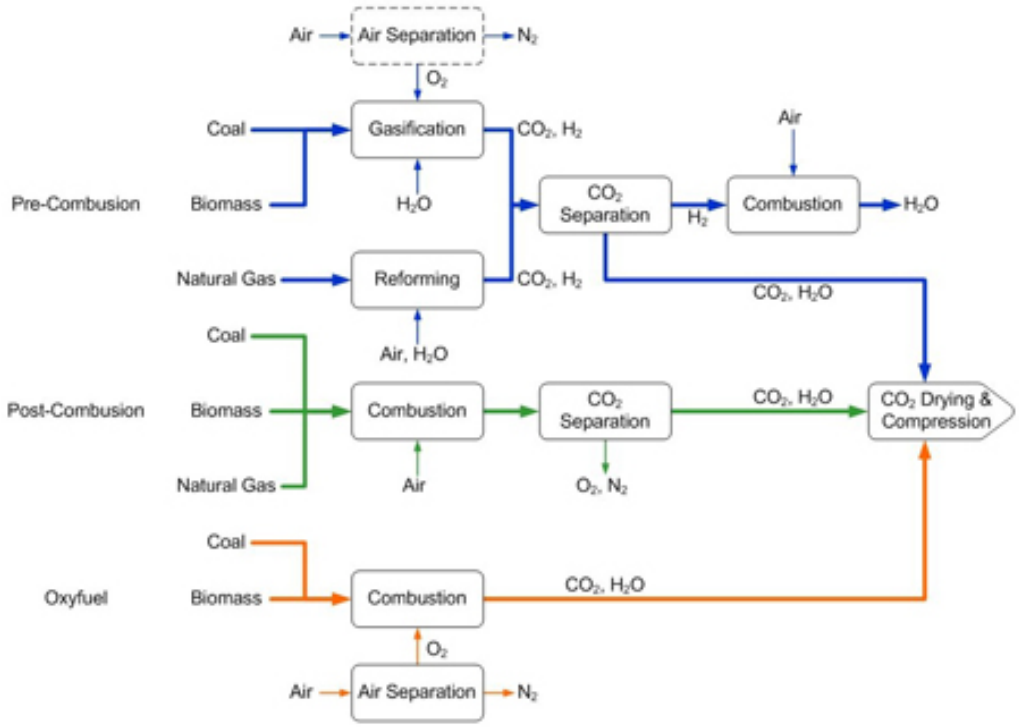

Figure 1.1: Overview of the three main routes for CO_2-capture (CCS, 2015)

1.2.2 Post-Combustion

In a post-combustion CO_2-capture processes a carbon-containing fuel is combusted in air, producing an exhaust gas with the major components being nitrogen (N_2) and CO_2. CO_2 is separated from this gas. The CO_2 concentration in such exhaust gases is relatively low, typically around 10-15% (Kanniche et al., 2010), depending on type of industry and fuel.

1.2.3 Oxyfuel

In oxyfuel there is no direct separation of CO_2, but rather a separation of oxygen from air. The fuel is burned with almost pure oxygen, and with optimized stoichiometry of fuel and oxygen the exhaust-gas consist of mainly CO_2 and water vapor. Water is easily separated by phase-separation, and the product gas is purified CO_2(Kanniche et al., 2010) which can be sent to compression and storage.

1.3 Capture technologies

There are several technologies available for CO_2 capture, and the aim of current research is to reduce the overall energy consumption related to the capture process. The best suited separation technology will depend on several factors, such as CO_2 concentration and composition of the gas mixture, downstream use of the product gases, impurities in the gas and temperature and pressure of the inlet gas stream. Until present the most studied capture technologies are chemical absorption, adsorption, cryogenic separation and separation by membranes (Yang et al., 2008). This report studies chemical absorption technology.

1.3.1 Absorption technology

Chemical absorption of a gas into liquid is a two-step process. In the first step the gas is dissolved into the liquid phase. The mechanism is shown for CO_2-gas in Equation (1.1).

$$CO_2(g) \overset{H_2O}{\rightleftharpoons} CO_2(aq) \tag{1.1}$$

The dissolved CO_2, CO_2(aq), then reacts with chemicals dissolved in the liquid. As the dissolved CO_2 reacts, the equilibrium in Equation (1.1) is shifted towards the right hand side, and more gaseous CO_2 is allowed to be dissolved.

1.3.2 CO_2 absorption technology

At present, the most developed technology for CO_2-capture is post-combustion absorption by amines(Figueroa et al., 2008a). An illustration of the process is given in Figure 1.2. The flue gas, containing CO_2, flows to the absorber tower, and is contacted with amines solved in water. The temperature in the absorption tower typically around 40-60 °C. The amines will react selectively with CO_2 and form water-soluble compounds. The liquid outlet from the absorber, which is enriched in CO_2 (henceforth referred to as "CO_2-rich solvent"), is heat-exchanged with the CO_2-lean solvent, and taken to the stripper/desorber section. The CO_2-rich solvent is heated in a reboiler to a higher temperature, typically around 120-140 $°C$. At high temperature the

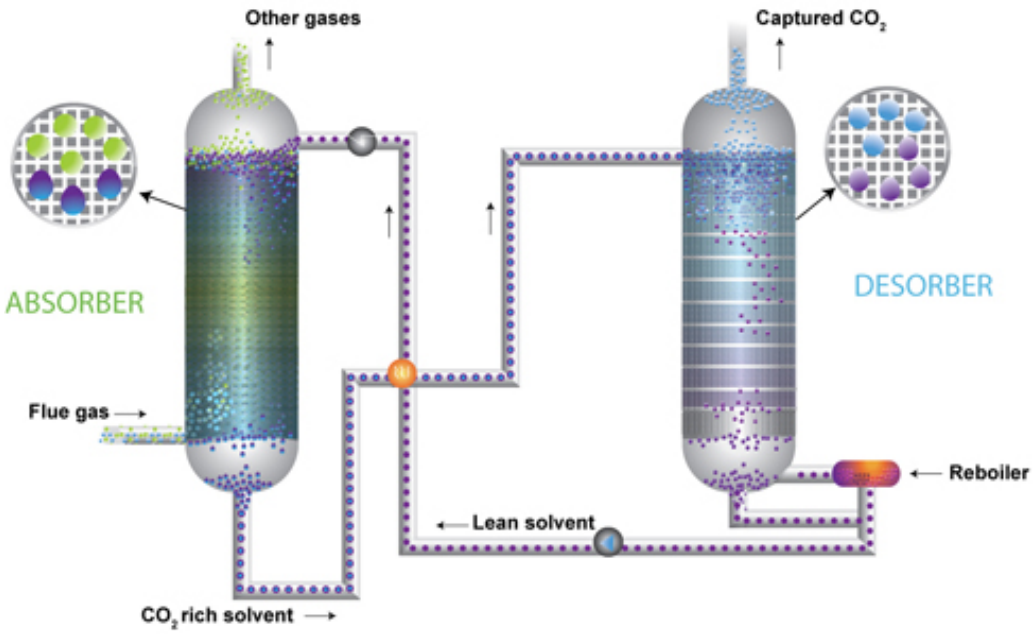

Figure 1.2: Illustration of CO_2 capture by absorption (CO2crc, 2015)

exothermic absorption-reaction is reversed and CO_2 is desorbed from the liquid phase. CO_2 exits the stripper as high purity CO_2-gas. The regenerated solvent, lean on CO_2, is circulated back to the absorber to perform a new round of CO_2 absorption. One important property of an absorption system is the loading, α, which is a measure of how many moles of CO_2 the system can absorb per mole of amine. α is given as

$$\alpha = \frac{n_{CO_2}}{n_{amine}} \tag{1.2}$$

Another parameter which is used to describe the overall performance of a CO_2 absorption/desorption process is *cyclic capacity*, Q (McCann et al., 2008). The cyclic capacity is the total of CO_2 which is removed per liter of solvent, as seen in Equation (1.3). The cyclic capacity takes into account that there will be CO_2 remaining in the lean solution after the stripper, and is given as

$$Q[\frac{moleCO_2}{L_{solvent}}] = C_{amine} \times (\alpha_{rich} - \alpha_{lean}) \tag{1.3}$$

where α_{rich} is the loading of the CO_2-rich solution going out of the absorber and α_{lean} is the loading of the lean solution, entering the absorber. C_{amine} is the the molar concentration of amine in the original solution, given as mol amine per liter. The energy consumption in the absorption capture process

is mainly related to the stripper section, where steam is used to heat the rich solvent. To reduce the need for steam the solvent is desired to have a reasonably low heat of absorption, but without compromising the other system properties (Arshad et al., 2013). Research is continuously performed to develop environmentally friendly solvents which have high cyclic capacity, high reaction rates, low solvent degradation and low energy consumption.

The chemicals most used in conventional absorption technology for CO_2 capture are amines. Amines are a group of organic compounds which have one or more nitrogen groups attached. Amines used for CO_2 absorption are divided into three groups, depending on the number of functional groups attached to the nitrogen atom. They are primary-, secondary- and tertiary amines, with respectively one, two and three functional groups attached to the nitrogen (Carey and Sundberg, 2007) (Vogel, 1974). The functional group(s) will impact the properties of the amines, and they will for instance differ with respect to reaction rate and heat of absorption(Arshad et al., 2013). The amine groups are illustrated in Figure 1.3. The primary and secondary amines form carbamates when reacted with CO_2. They are very reactive, with high reaction rates and relatively high heat of absorption(Sartori and Savage, 1983). The reaction between CO_2 and a carbamate-forming amine is shown in Equation (1.4), here illustrated with a secondary amine. *R, R'* and *R"* are different functional groups.

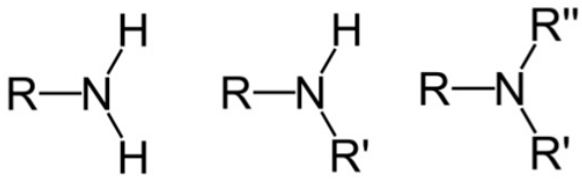

Figure 1.3: Illustration of primary, secondary and teriary amines. R represents a functional group.

$$CO_2 + 2RR'NH \rightleftharpoons RR'NCOO^- + RR'N^+H_2 \tag{1.4}$$

As seen in Equation (1.4) the stoichiometry limits the loading of a carbamate-forming amine to 0.5, as two moles of amines are needed per mole of CO_2. Tertiary amines have no hydrogen available for carbamate-formation, and thus follow other reaction mechanisms. The reaction between a tertiary

amine and CO_2 forms bicarbonate ions as shown in Equation (1.5).

$$CO_2 + R'R''R''N \overset{H_2O}{\rightleftharpoons} HCO_3^- + R'R''R''N^+H \tag{1.5}$$

Tertiary amines typically have lower heat of reaction, and a lower reaction rate than the carbamate-forming amines(Sartori and Savage, 1983)(Crooks and Donnellan, 1990). The stoichiometry of the reaction between tertiary amines and CO_2 provides a theoretical loading capacity of 1(Vaidya and Kenig, 2007).

Neither of the primary- secondary- or tertiary amines provide ideal properties as solvents for a CO_2-absorption process. To improve the overall performance of a CO_2 capture plant, a method of increasing interest is to use mixed amine systems. In such systems the higher loading capacity of the tertiary amines is combined with the high reaction rates of the primary- and secondary amines. The energy requirement for regeneration of solvents is reported to be reduced in such systems (Hagewiesche et al., 1995). Recently new solvents has been found which, when mixed at specific blends, form two phases when reacted with CO_2. The solvent mixture is present as one liquid phase when unloaded, and when a certain CO_2 loading is reached the solution splits into two liquid phases, one phase more rich in CO_2 than the other. In a capture process the idea for such a system is to only send the richest phase to the stripper section. The rich phase will contain large amounts of CO_2, thus reduce the liquid flow and reduce the need for heating which lead to savings in energy per kilo CO_2 captured(Pinto, 2014).

1.4 Heat of reaction

One factor which is directly related to the energy consumption in the stripping section is the heat of reaction. Heat of reaction, or in this work equivalent to *heat of absorption*, will be determinative for the energy required to desorb the CO_2 from the rich solvent in the stripper(Arshad et al., 2013). Heat of reaction, ΔH_{rx}, is the change in enthalpy of a chemical reaction that occurs at constant pressure (Kjelstrup and Helbæk, 2006).

$$\Delta H_{rx} = \sum_{i=1}^{n} H_{reactant,i} - \sum_{i=1}^{n} H_{products,i} \tag{1.6}$$

$\sum_{i=1}^{n} H_{reactant,i}$ is the sum of enthalpy for all reactants, and $\sum_{i=1}^{n} H_{products,i}$ is the sum of enthalpy for the products. In a closed system at constant pressure the enthalpy change is equal to generation or consumption of heat. The change in heat is a function of mass, heat capacity of the mass and temperature difference before, T_{before}, and after, T_{after}, the reaction has occurred. Thus, the expression is

$$\Delta H = q = \cdot Cp \times (T_{before} - T_{after}) \tag{1.7}$$

Heat of reaction can be experimentally measured in a reaction calorimeter, an isolated system capable of measuring temperature, pressure and the supplied heat as a function of time.

1.5 Project description

This work is a part of the 3rd Generation Membrane Contactor (3GMC)-project at NTNU. The scope is to investigate new solvents for use in a combined absorption/membrane system. Two solvents will be investigated which at specific blends and concentrations form two liquid phases within a specific range of CO_2-loadings (Ciftja et al., 2015). The solvents are the tertiary alkanolamine 2-diethylamino-ethanol (DEEA), and the diamine 3-methylamino-propylamine (MAPA), which has one primary and one secondary amine group. Due to the two amine groups per molecule in a diamine, MAPA has a higher theoretical loading than primary- and secondary amines with only one amine group per molecule. The structure of DEEA- and MAPA-molecules are presented in Figure 1.4.

A blend of the two amines combines the high absorption rate provided by the primary- and secondary amine, MAPA, and high loading capacity and lower heat of absorption, provided by the tertiary amine, DEEA. The work will to a large extent involve measurements of the heat of absorption in DEEA-MAPA systems, and investigation of the effect on heat of absorption when two phases form. The well-established solvent Monoethanolamine (MEA) is tested in the same calorimeter as a reference to verify the results from this work. In addition to heat of absorption data, VLE-data is also produced. In addition, a series of simple experiments are performed to study for which loadings the two phases in a DEEA/MAPA-system are present.

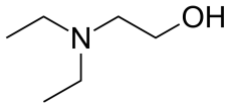

(a) DEEA

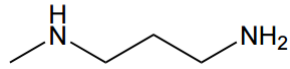

(b) MAPA

Figure 1.4: Molecular structures

1.6 Relevant literature data

Measurement of heat of absorption for amine-water-CO_2 system has been well researched, and the performance of a number of amines are studied(Kim et al., 2013)(Kim and Svendsen, 2007a) (Mathonat et al., 1998) (Schäfer et al., 2002). At present the most investigated amine is MEA.

1.6.1 MEA

The performance of absorption of CO_2 in MEA is studied and data are available in the open literature. This includes data for heat of absorption (Kim et al., 2014)(Kim and Svendsen, 2007b)(Arshad, 2014)(Kim et al., 2011)(Langé et al., 2015) which makes MEA a good item for comparison of the amines studied in this work. The most investigated concentration of MEA is 30 weight percent(wt%). Data from Kim (Kim, 2009) and Arshad (Arshad, 2014) for a concentration of 30wt% MEA will be used for comparison in this report.

1.6.2 DEEA + MAPA

A number of articles are available in the open literature on CO_2 capture in mixed solvent systems of DEEA and MAPA (Monteiro et al., 2015)(Hartono et al., 2013)(Pinto et al., 2014b)(Pinto, 2014)(Pinto et al., 2014a)(Arshad et al., 2013)(Liebenthal et al., 2013).Experimental data from measurements of Vapor/Liquid Equilibrium (VLE), kinetics and screening of two-phase forming mixtures has been published. Heat of absorption is measured by Arshad (Arshad et al., 2013) for a selection of DEEA-MAPA-systems, where one of his systems is reported to form two phases when loaded with CO_2. Arshad also presents data on heat of absorption of CO_2 in DEEA-water- and MAPA-water-systems. Data from Arshad will be used for comparison with results obtained in this work. (Kim, 2009) has performed measurements on

heat of absorption in the very same calorimeters as are used in this work and presents data for MEA and different blends of DEEA/MAPA.

Previous work in the 3GCM-project has involved screening of different concentrations and ratios of DEEA and MAPA(Ciftja et al., 2015). The screening-results reveal which blends of DEEA-MAPA which form two phases upon absorption of CO_2. The results are used as a base to select blends of DEEA and MAPA for studies in this project work.

Experimental VLE-data for a selction of blends of DEEA and MAPA is reported by Rennemo (Rennemo, 2015b), at temperatures 40, 80 and 120 °C. VLE-data has also been published by Pinto for different DEEA-MAPA-systems, and he proposes a model to describe their thermodynamic behaviour(Pinto, 2014). The data from Rennemo will be used for comparison to results obtained in the experimental work in this report.

Chapter 2

Experimental procedure

2.1 Chemicals

The chemicals used in the experimental part of this project are summarized in Table 2.1. The Material Safety Data Sheets (MSDSs) for the chemicals used in this project are attached in Appendix C. De-Ionized water (DI-water) is used for preparation of the solutions. In preparation of the solutions, water and chemicals are measured by weight. Small amounts of Barium Chloride,

Table 2.1: Chemicals used in experimental work

Chemical	Abbreviation	CAS-number	Purity
Carbon Dioxide	CO_2		99.99%
Monoethanolamine	MEA	141-43-5	99%
2-(diethylamino)-ethanol	DEEA	100-37-8	99.5%
3-(methylamino)-propylamine	MAPA	6291-84-5	98%

Sulphuric Acid and Sodium Hydroxide of low concentrations are used for analysing samples.

2.2 Performed experiments

2.2.1 MEA - Validation of experimental data

The first step in the experimental work was to validate that data obtained from the calorimeter match data from previous work available in the literat-

ure. MEA-solutions with a concentration of 30wt% were used. An overview of the MEA-experiments is presented in Table 2.2, where A and B denotes respectively first and second parallel at the same temperature.

Table 2.2: Experiments performed with 30wt% MEA.

Temp. [° C]	Experiments	
40	MEA30wt%-40-A	
80	MEA30wt%-80-A	MEA30wt%-80-B
120	MEA30wt%-120-A	

2.2.2 DEEA-MAPA systems

Six different blends of DEEA and MAPA are studied. Some remain as one liquid phase, and some form two liquid phases when reacted with CO_2. The choice of solvent mixtures is based on previous measurements of phase formation performed by Ciftja (Ciftja et al., 2015). The blends of solvents studied in this work are summarized in Table 2.3. The molarities are given as moles/kg solution.

Table 2.3: Mixed blends of DEEA and MAPA

	System	T[°C]	Experiment abbreviation	
One Phase	3M DEEA+1.5M MAPA	40	3D1.5M-40-A	3D1.5M-40-B
		80	3D1.5M-80-A	
		120	3D1.5M-120-A	
	3M DEEA+2M MAPA	40	3D2M-40-A	3D2M-40-B
		80	3D2M-80-A	3D2M-80-B
		120	3D2M-120-A	3D2M-120-B
	1M DEEA+5M MAPA	40	1D5M-40-A	1D5M-40-B
		80	1D5M-80-A	1D5M-80-B
		120	1D5M-120-A	1D5M-120-B
Two Phases	3M DEEA+3M MAPA	40	3D3M-40-A	3D3M-40-B
		80	3D3M-80-A	3D3M-80-B
		120	3D3M-120-A	3D3M-120-B
	3M DEEA+3.5M MAPA	40	3D3.5M-40-A	3D3.5M-40-B
		80	3D3.5M-80-A	3D3.5M-80-B
		120	3D3.5M-120-A	3D3.5M-120-B
	3.5M DEEA+3.5M MAPA	40	3.5D3.5M-40-A	

The abbreviations for each experiment given in Table 2.3 are further used in the report. Abbreviations are also used to refer to the different blends, where D is short for the molarity of DEEA and M is short for the molarity of

MAPA. The majority of the blends are tested two times at all temperatures to verify the reproducibility. The first parallel is labelled A, and second parallel is labelled B. Solutions for each of the parallels are prepared in separate batches to mitigate sources of error related to the solution preparation. The 3.5M MAPA+3.5M DEEA system is not previously tested by Citja, but was tested to see how an increase in total amine concentration affects the system properties. This system is performed once at 40°C.

2.3 Apparatus and Experimental Procedure

Experiments are performed in two separate, but almost similar, CPA-122 calorimeters from ChemiSens AB. A picture of calorimeter 2 is shown in Figure 2.1. The calorimeters are jacketed reactors which hold a volume of 2000cm^3, mechanically agitated and with the capability of measuring heat flow in the system, temperature and total pressure as a function of time. The reactors are operated at isothermal conditions, meaning the temperature is kept constant. Heat flow is measured by integration of supplied heat to the circulating fluid in the jackets to maintain a set temperature in the reactor. The reactors are suitable for operation at pressures between -1 and 100 bar, at temperatures ranging from -20 to 200°C. The terms 'calorimeter' and 'reactor' are used more or less arbitrary throughout this work.

A photo of the experimental set-up is shown in Figure 2.2. The equipment is connected to a computer, running the software "ChemiCall" from ChemiSens AB (ChemiSens, 2015). The software produces a log file with all measured parameters as a function of time, and also provides graphs and calculation tools.

The calorimeters are separate reactor systems, but share the same vacuum cylinder and CO_2-cylinders, marked as respectively 5 and 2a/b in Figure 2.2. Experiments can be run simultaneously, but the CO_2 loading sequence can only be performed in one system at a time. Pressure and temperature in the CO_2-cylinders are logged by the software for both calorimeter 1 and 2. Calibration parameters were set in both computer programs, but values of pressure and temperature in the CO_2-cylinder were measured to be slightly different. To avoid differences between the results of experiments performed in the two calorimeters it was decided to read values from the computer program for calorimeter 2 for both calorimeters. The experiments are performed at three different temperatures; at T=40°C, 80°C and 120°C. 40°C is chosen because it is a typical temperature in the absorption column, and 120°C is

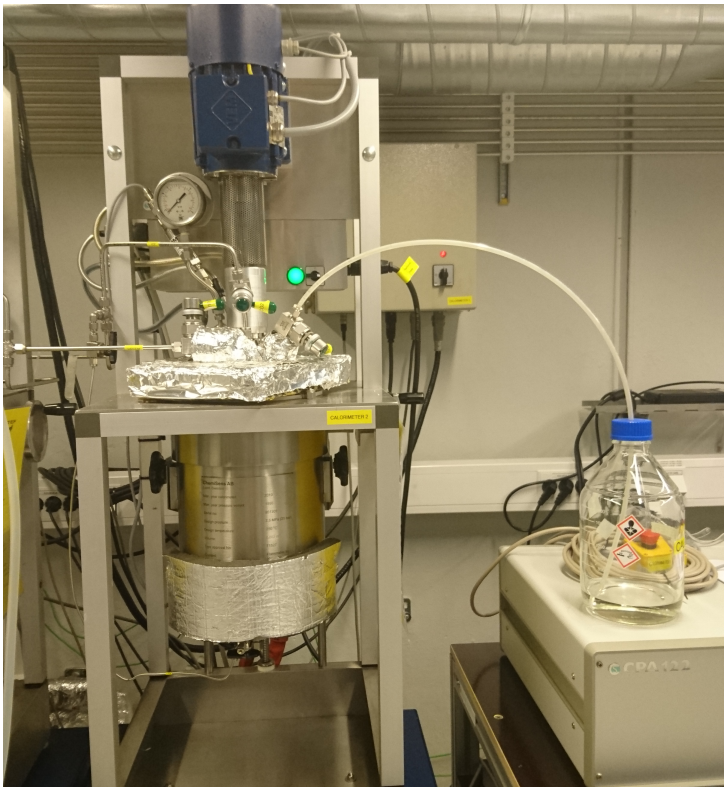

Figure 2.1: Calorimeter CPA-122 prepared for measurements

chosen as a typical temperature in the stripper column. 80°C is included to gain a better understanding of the behaviour of the overall CO_2-capture process.

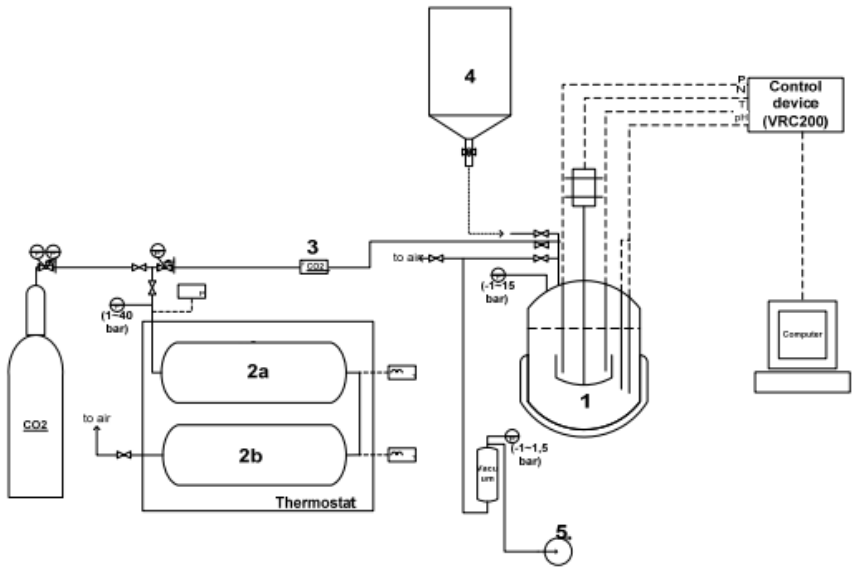

Figure 2.2: Experimental set-up for a CPA-122 calorimeter (Kim, 2009). 1- The reactor calorimeter; 2a and 2b- CO_2 cylinders; 3- Mass flow controller for measuring of CO_2 flow; 4- Amine solution feed bottle (manually handled); 5- Vacuum pump

2.3.1 Start-up of experiment

Approximately 1.5 L of the solution is prepared and transferred to a 2L feed bottle (Marked '4' in Figure 2.2). The system is switched on, including the circulation unit for the jacket fluid, control box, the PC and computer-software. The vacuum cylinder is evacuated, and the valves leading to the reactor (1) are opened. The reactor is evacuated; the pressure in the reactor is reduced to around 0.03bara or lowest possible. A tube connects the top of the reactor (1) and the solution feed bottle (4). The tube end in the solution feed bottle is held into the solution, and the vacuum in the reactor the liquid into the reactor, approximately 1.3 L. The weight of the bottle is noted before and after the solution is transferred to the reactor, and the total mass of solution in the reactor is calculated. The reactor is again evacuated by opening the valves to the vacuum cylinder for about 20-30 seconds to remove air and de-gas the solution. Temperature is set in the computer software and the stirrer is initiated. The system is left for minimum one hour to allow the system to reach equilibrium state.

2.3.2 Calibration

The ChemiSens measurement system measures the enthalpy difference between the inlet and the outlet of a circulated fluid in the jacket surrounding the reactor. At equilibrium the enthalpy difference is assumed to be equal to the enthalpy change inside the reactor. The equation for calculation of enthalpy change is derived from Equation (1.7) in Section 1.4, and is given as

$$\Delta H = \frac{dM}{dt} C_p \times (T_{in} - T_{out}) \tag{2.1}$$

The measured parameter T_{in} is the temperature of the fluid going into the jacket and T_{out} is the temperature of the fluid out of the jacket. They are measured parameters. $\frac{dM}{dt}$ is the flow-rate of the circulating fluid and C_p is the heat capacity of the fluid. The product $\frac{dM}{dt}C_p$, also termed 'FlowCP', is the only system parameter which needs to be calibrated. The calibration sequence is performed at each of the temperatures 40, 80 and 120 $°C$, with 30wt% MEA inside the reactor. In the computer software a predetermined power is turned on, termed *calibration power*. The calibration power is assumed to be a true value, and the FlowCP is adjusted such that the measured total power matches the value of the calibration power. The calibration sequence is performed several times at each temperature, yielding a serie of FlowCP-values. The values of the measured FlowCPs are presented in Appendix A.

This calibration sequence was performed in the beginning of the working period, and the same calibration values are used in all further experiments. The calibration-values are assumed independent of the fluid inside the reactor. As the heat of absorption is found by measuring the *supplied power* to keep the temperature at the value, information about the heat capacity of the fluid inside the reactor is not needed.

2.3.3 Feeding of CO_2

The CO_2 storage cylinders (2a and 2b in Figure 2.2) are filled with CO_2, and fed to the reactor in batches. This is manually controlled by the computer software and by opening/closing valves. The pressure and temperature in the CO_2-cylinders are noted before and after the addition of CO_2, and the CO_2 flow is controlled by a flow-controller. This way the amount of CO_2 added to the reactor is calculated in to ways; 1) integration of the CO_2 flow over

time, measured by the flow-controller(3), and 2) calculations by the Peng-Robinson equation of state using information about pressure difference and temperature in the CO_2 cylinders. Peng-Robinson equation of state will be described in Section 2.5.2. Each of the calorimeters has its own flow-controller, which has been previously calibrated and are assumed to show results within an acceptable range of error.

A portion of CO_2 is fed into the reactor, and the system is allowed to reach a new steady-state. All parameters should become stable, such as the reactor temperature -and pressure, total power and pressure in the CO_2 cylinders. A new portion of CO_2 is added, and the system is allowed to reach a third equilibrium state. The addition of portions of CO_2 is continued until the reactor pressure increases significantly, indicating that the system is saturated or coming close to the maximum loading possible at the specific temperature. At this point physical absorption is dominating, and the loading is above the range which is relevant in a CO_2-capture process.

2.3.4 Sampling and determination of loading

When the system has reached equilibrium after addition of the last portion of CO_2, a sample is collected from the liquid phase. A cylinder with a volume of 100mL is first evacuated, weighed, and filled with approximately 50mL of unloaded solvent. The cylinder with unloaded solution is weighed. A sample is collected from the bottom of the reactor, transferred through a short pipeline, and added to the cylinder. The cylinder is weighed again. The lean solvent is mixed with the sample to prevent physically absorbed CO_2 to leave the sample as the pressure is decreased. The excess of solvent will chemically absorb the physically solved CO_2 and hold it in the liquid sample.

Two set of analysis are performed to determine the loading in the sample; the concentration of amines and the concentration of CO_2 in the sample.

2.3.5 Amine analysis

Approximately 0.2mL of sample is added to 50mL of DI-water, and the samples are titrated with 0.1M H_2SO_4 in an automatic titrator. The equation for determination of moles of amine groups per kg solution is given in Equation (2.2). The density of HCl is assumed to be 1kg/L. A hydrogen

proton reacts with amine functional groups with the stoichiometry 1:1.

$$C_{amine}\left[\frac{\text{mol}_{amine-groups}}{\text{kg}_{sample}}\right] = \frac{V_{H_2SO_4}[\text{mL}] \times 0.2(\frac{\text{mole}H^+}{kg})}{\text{m}_{sample}[g]} \tag{2.2}$$

C_{amine} is the concentration of amine groups given as moles per kg sample. $V_{H_2SO_4}$ is the volume of sulphuric acid needed to neutralize the solution. m_{sample} is the mass of sample. Two parallels are run for each sample.

2.3.6 CO_2 analysis

Each sample is analysed twice, and up to four samples are analysed in each round of analysis. In addition, a solution is prepared without adding sample, referred to as the 'blank' sample. For each parallel an Erlenmeyer flask is filled with 25mL BaCl, 50mL of DI-water and 0.8mL of sample. The sample weight is recorded (except from the blank sample). The solutions are boiled for 4 minutes and then cooled to room temperature. The purpose is to precipitate $BaCO_3$ by the following reaction:

$$Ba^{2+} + CO_2 + 2OH^- = BaCO3(s) + H_2O \tag{2.3}$$

The solutions with precipitation are vacuum filtrated. The filters with precipitation are transferred to new beakers and DI-water and known amount of HCl are added to each of the beakers. The beakers are stirred with magnets for a while to dissolve the solids. $BaCO_3$ dissolves in acid by the following reaction:

$$BaCO_3 + 2HCl = BaCl_2 + CO_2 + H_2O \tag{2.4}$$

When all $BaCO_3$ is dissolved the solutions are titrated with a 0.1N $NaOH$ solution in an automatic titrator. The CO_2 concentration is calculated from the equation:

$$C_{CO_2} = \frac{1}{20} \times \frac{[m_{HCl}[g] - V_{NaOH}[ml] - m_{BlankHCl}[g] + V_{BlankNaOH}[ml]]}{m_{Sample}[g]} \tag{2.5}$$

C_{CO_2} is the CO_2 concentration given as moles CO_2 per kg solution. V_{NaOH} is the volume of base needed to react with the CO_2 in the solution, $V_{BlankNaOH}$ is the amount of $NaOH$ needed in the blank solution. The blank solution is used as a reference for "zero" CO_2 in the solution. m_{HCl} and $m_{BlankHCl}$ are the amounts of acid added to a solution with sample and the blank solution,

respectively. For Equation (2.5) to be valid the density of $NaOH$ must be 1 kg/L.

2.3.7 Observations of loaded solutions

From around halfway in the experimental executions the final loaded solutions were stored in a glass bottle for a day or so, and pictures were taken. The idea was to observe colours, viscosity and, if present, the fraction of each of the two phases.

2.4 Observations of two-phase formation

The calorimeters used in the heat of absorption experiments are made of metal, and do not allow for observations while the experiments are running. Thus, the point when two phases first occur is unknown. An attempt of estimating for which loading two phases first occur, some simple experiments are performed. A glass cylinder is filled with a known amount of lean solution and placed on a weight. A tube, connected to a CO_2-container, is immersed into the liquid. The scale is tared, and CO_2 is fed to the system in batches. CO_2 is bubbled through the liquid, which provides agitation in the cylinder. The weight after each batch of CO_2 is noted, and observations are made. The difference in weight is assumed to be CO_2, absorbed in the liquid, and loading can be calculated. The height of each of the phases are measured to study the fraction of phases as a function of loading. This experiment was performed once for each of the two-phase forming systems.

The experiment was repeated the solutions 3D3M and 3D3.5M, but now directly to a loading where two phases are present. The height of each of the phases are noted at room temperature (T≈22°C), the solutions are heated up to T=50°C before the height of the phases are measured again.

2.5 Calculations

2.5.1 Heat of absorption

The calorimeter measures the total power which is needed to keep the system at a set temperature. When a reactant is introduced to the system, heat

is released or consumed, depending on the type of reaction. The reaction between CO_2 and amines studied in this report are exothermic, meaning that heat is released when CO_2 is supplied, and the total power supplied is thus in the form of cooling. A log-file from one of the experiments produced by the ChemiCall software is shown in Figure 2.3.

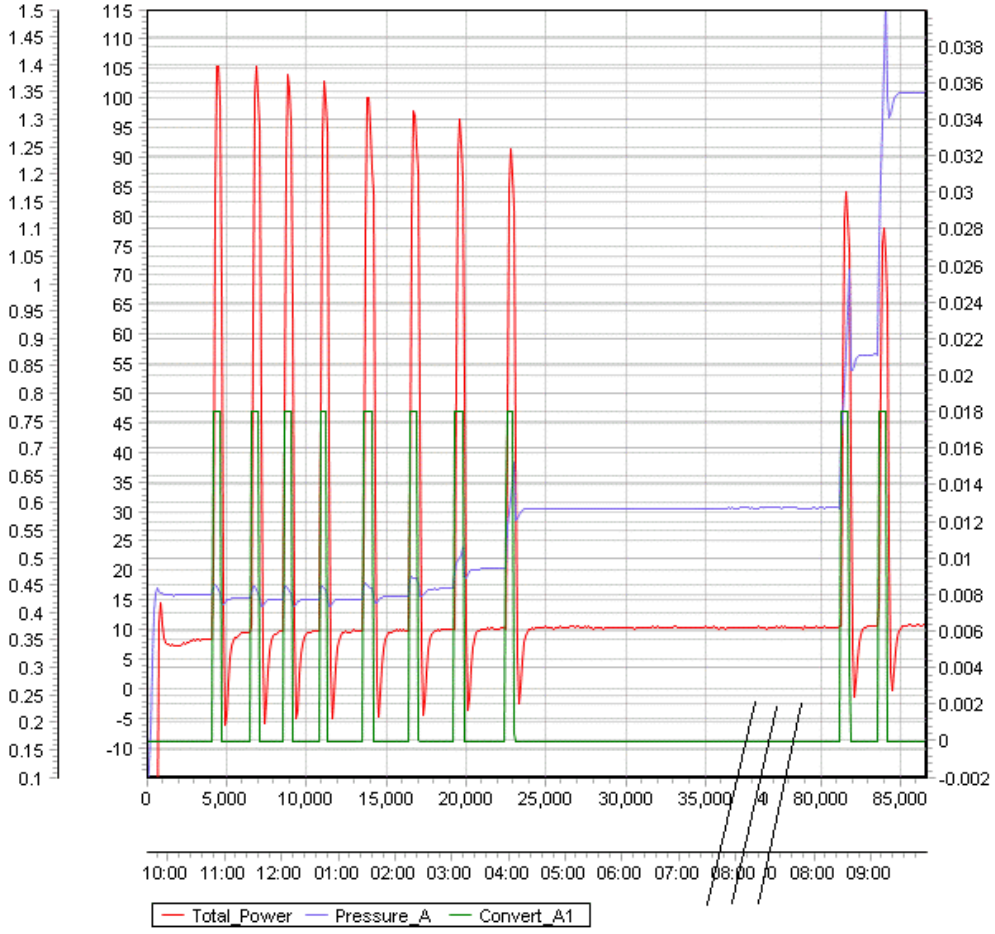

Figure 2.3: Screenshot from the logfile for experiment 3D3M at 80 °C, showing the total power as a function of time. Total Power is the power supply [W], Pressure_A is the total pressure in the reactor [bar], and convert_A1 is the CO_2-flow through the flowmeter[L]. The x-axis is truncated due to no activity.

Between each CO_2-loading the system is assumed to be at steady state when temperature, pressure and the supplied power are stable. The heat of absorption is found by integrating the supplied power between two points where the system is at equilibrium before and after a CO_2-loading. A line

is drawn between the adjacent points on the time-line, and serves as the baseline of integration. This baseline is located at a value above zero because of continuously supplied heat to compensate for heat loss to surroundings. The advantage of the baseline is that it acts as a new "zero-line", and the integrated power will be the *additional* power supply, related to the heat of reaction.

2.5.2 Peng-Robinson equation of State

Peng-Robinson equation of state is used to calculate the amount of CO_2 transferred from the CO_2-cylinders to the reactor, based on temperature and pressure in the cylinders before and after the addition. The Peng-Robinson equation of state was proposed in 1976, and is reported to be superior for prediction of VLE in hydrogen/nitrogen-mixtures, and relatively accurate correlations in gas mixtures even at high pressures(Peng and Robinson, 1976)(Jaubert and Mutelet, 2004). The Peng-Robinson equation, explicitly in pressure, is given as

$$p = \frac{RT}{V_m - b} - \frac{a\alpha}{V_m^2 + 2bV_m - b^2} \tag{2.6}$$

where

$$a = \frac{0.45724R^2T_c^2}{P_c},$$

$$b = \frac{0.07780RT_c}{P_c},$$

$$\alpha = (1 + (0.37464 + 1.54226\omega - 0.26992\omega^2)(1 - T_r^{0.5}))^2$$

and

$$T_r = \frac{T}{T_c}$$

ω is the acentric factor for a specie, P_c is the critical pressure, V_m is the molar volume, R is the gas constant, T_c is the critical pressure, and T is the measured temperature.

2.5.3 VLE-calculations

The work in this report does not include extensive studies of VLE. However, the total pressure is logged for all experiments, which allows for an estimation of VLE-data. After evacuation at start-up of the experiment only negligible

amounts of CO_2 is present. Further it is assumed that all increase in total pressure in the reactor is due an increase in CO_2 partial pressure. The equation for calculating CO_2 partial pressure, p_{CO_2} is then

$$p_{CO_2} = P_{tot} - P_0 \tag{2.7}$$

where P_0 is the pressure after evacuation and P_{tot} is the total pressure measured in the calorimeter after each loading. As previously described the amount of CO_2 added in each loading is found by two methods, and is assumed to be known parameter. The loading in the liquid phase is predicted based on mass balance in added CO_2, and CO_2 present in gas phase.

Chapter 3

Results and discussion

3.1 Presentation of data and general concid-erations

The deviation between the flow meter-readings and values calculated by Peng-Robinson-method are inside a range of ±4%, with the majority of the loadings deviating in the range of ±2% in calorimeter 2. With few exceptions the flow meter readings show slightly higher values than calculations by Peng-Robinson. In calorimeter 1 the flow meter typically gives values which are 5-10% lower than values calculated by Peng-Robinson equation of state. Determination of added CO_2 by two methods were originally thought as a way to validatate that each of the methods show correct values found by each of the methods. The fact that the flow meter shows consistently lower values than Peng-Robinson calculations in calorimeter 1 and the trend is slightly opposite in calorimeter 2 indicates that at least one of the flow meters are poorly calibrated. Calorimeter 1 and 2 are connected to the same CO_2-cylinder, and the pressure and temperature in the cylinders are read from calorimeter 2 for experiments in both calorimeters. To avoid differences related to which of the calorimeters the experiments are performed in, it was chosen to use Peng-Robinson as the base for calculations of added CO_2 for both calorimeters. Thus data presented in this report is consequently based on calculations by Peng-Robinson equation of state.

The heat of absorption is calculated as the total heat of absorption measured in one interval divided by the total moles of CO_2 added in the same interval. Thus, heat of absorption is reported as energy per unit CO_2, as an average over each interval. The manual graphical integration is performed three

Table 3.1: Operating pressure at the different operation temperatures

T [°C]	Start pressure [bar]	End pressure [bar]
40	0.073-0.089	0.433-0.765
80	0.380-0.403	1.005-1.793
120	1.899-1.950	2.540-3.692

times per interval, and the average of the three values is used in the results. The heat of absorption is plotted as a function of loading at the *end* of each interval. This is equivalent to results reported by (Kim et al., 2014) and (Arshad, 2014), and to allow for easy comparison it was chosen to use the same presentation. The amount of CO_2 added in each loading varies slightly, and single points where the amount of added CO_2 is significantly smaller or larger than the adjacent points will shift the loading down or up, respectively. A better option could be to present the data as a function of the *average* loading over an interval.

The pre-experiment evacuation was performed at room-temperature for all experiments. The total pressure in the reactor increases for increasing temperature, and typical operating pressures at the three temperatures are summarized in Table 3.1. All experiments with DEEA-MAPA are summarized in Table 3.2, with observations and comments from the experiment.

As described in Section 2.2.2, the systems were chosen based on screening experiments by (Ciftja et al., 2015). The two blends which were observed to give two phases by (Ciftja et al., 2015) (3D3M and 3D3.5M) were observed with two phases also in this work for at least one of the operation temperatures, as shown in Table 3.2. 3D1.5M, 1D5M and 3D2M all remained as one phase at the final loading, consistent with the results from Ciftja. A further discussion of two phase formation follows in Section 3.5. Ciftja has calculated the cyclic capacity of several DEEA-MAPA blends, based on specific loadings of rich phase and lean phase for each blend. A temperature of 40°C is used to represent the absorption column (rich loading) and 120°C to represent the desorption column (lean loading), similar to the temperatures in this work. The experiments in this work do reach the loadings used in calculations of cyclic capacities performed by Ciftja at relevant temperatures. Thus, the heat of absorption measurements in this work cover the range in loadings in the work by Ciftja, and could be used for estimation of energy consumption of the absorption/desorption process.

Table 3.2: Summary of performed experiments, with observations of unloaded- and loaded solutions. Colour, number of phases and comments from the experiment are included. The experiments marked with * are performed in calorimeter 1, all others are performed in calorimeter 2.

Experiment	**Colour: Unloaded**	**Colour: Loaded**	**# of phases**	**Comment**
MEA30-40-A	Blank	Blank	1	
MEA30-80-A	Blank	Blank	1	
MEA30-120-A	Blank	Blank	1	
MEA30-80B	Blank	Blank	1	Software breakdown, overheating and emergency cooling. Experiment continued.
3D1.5M-40-A	Blank	Blank	1	Not viscous
3D1.5M-80-B	Yellow	Blank	1	
3D1.5M-120-A	Yellow	Blank	1	
3D1.5M-40-B	Blank	Pink	1	Software breakdown. Not completed to high loading.
3D2M-40-A	Yellow	Pink	1	
3D2M-80-A	Yellow	Blank	1	
3D2M-120-A	Yellow	Blank	1	Forgot to re-evacuate, P_start=0.086bar
3D2M-40-B	Blank	Pink	1	
3D2M-80-B	Blank	Slightly pink	1	
3D2M-120-B	Blank	Blank	1	
1D5M-40-A	Blank	Light pink	1	
1D5M-80-A	Blank	Light pink	1	
1D5M-120-A	Blank	Blank	1	
1D5M-40-B	Blank	Pink	1	Very sticky
1D5M-80-B	Blank	Yellow	1	
1D5M-120-B	Blank	Yellow	1	
3D3M-40-A	Blank	Orange	1	
3D3M-80-A	Blank	Blank	1	
3D3M-120-A	Blank	Blank	2	Thin layer of new phase
3D3M-40-B	Blank	Light pink	2	Thin layer of new phase, less viscous than previous loaded solutions at 40.
3D3M-80-B	Blank	Slight yellow	2	Appoximately 1cm of upper phase
3D3M-120-B	Blank	Blank	2	Emergency cooling due to lack of oil.
3.5D3.5M-40-A	Slight yellow	Pink	1	Loaded solution was like glue.
3D3.5M*-40-A	Blank	Pink	1	Small leakage in first part of execution→ Pressure increase. Tightened bolt, experiment continued.
3D3.5M-80-A	Blank	Slight yelow	2	Very sticky loaded solution
3D3.5M-120-A	Slight yellow	Slight yellow	2	CO2-pipeline clogged in the part closest to the inlet of the reactor. Uneven CO2-flow.
3D3.5M*-40-B	Blank	Orange/pink	1	Leakage in first part of execution.
3D3.5M*-80-B	Blank	Slight yellow	2	
3D3.5M*-120-B	Blank	Blank	2	

3.1.1 Differences in integration values

The experimental procedure has some potential errors which may affect the final results in the heat of absorption measurements. The first, and probably the major source of error, is the integration of power in the computer software. This part of the procedure was described in Section 2.5.1. The integration is performed three times per interval, and the average of the three integrations is used in the results. By integrating several times the effect from having one bad value is reduced. As an example of the significance of deviations in integration values, the maximum, minimum and average values are plotted for experiment 1D5M-120-A, see Figure 3.1. The deviations between the three integrations values are in the same range as shown here in all experiments.

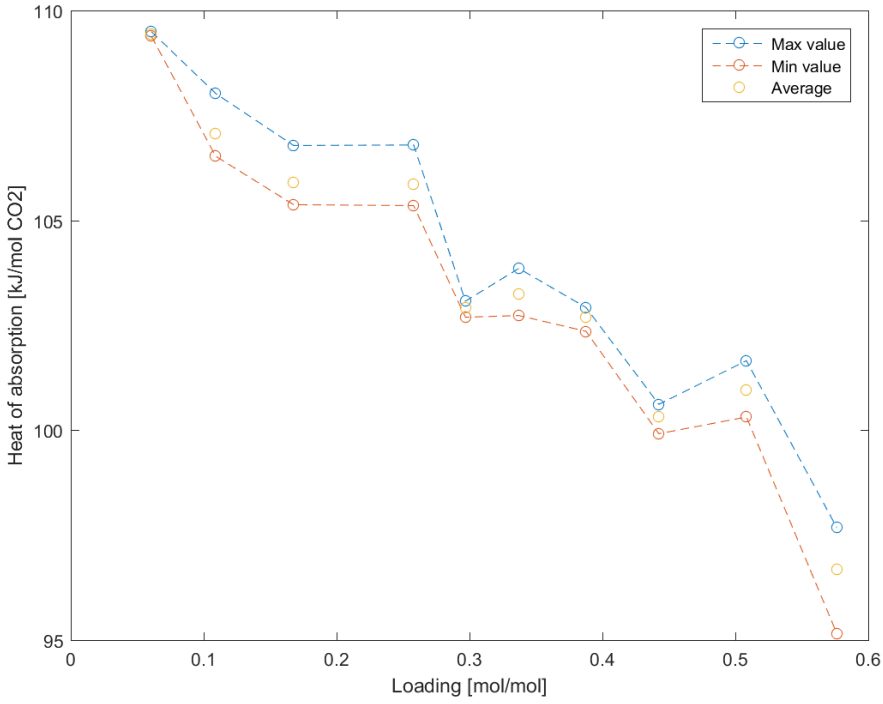

Figure 3.1: The maximum, minimum and average values of three integrations per CO2-loading-interval in experiment 1D5M-120-A.

The figure shows a deviation between maximum and minimum within the range of 1.5%. If it is assumed that the range between the maximum and minimum integration values are covering the true value of heat of integration in a specific interval, the error of the reported value is less than 1.5%.

However, as the integration is graphically, error of greater magnitude may occur.

3.2 Heat of absorption: MEA

The experimental data from the heat of absorption measurements of CO_2-absorption in MEA is presented in Figure 3.2-3.4. The figures include experimental data from previous work by (Kim et al., 2014) for reference comparison.

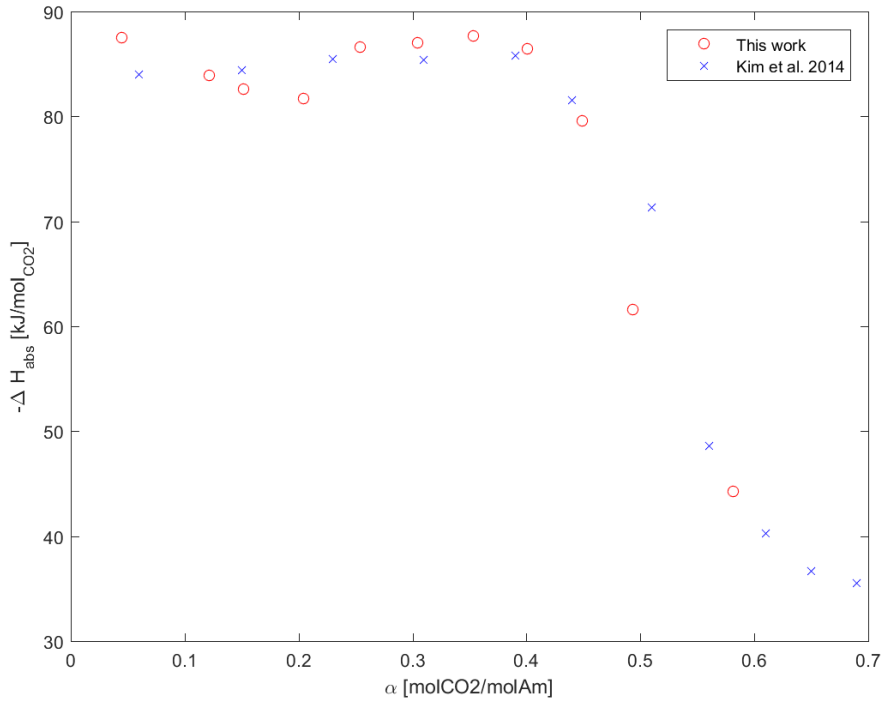

Figure 3.2: Measured heat of absorption in a 30wt% MEA solution at T= 40 °C. Experimental data from this work is compared to experimental data from previous work (Kim et al., 2014)

At 40°C, presented in Figure 3.2, data from this work show good agreement with data by (Kim et al., 2014). There are some outliers in data obtained in this work, but in general the heat of absorption is measured to be in the same range as found by Kim. (Arshad, 2014) has performed the same set of experiments with MEA, with similar results as obtained by Kim. Heat of

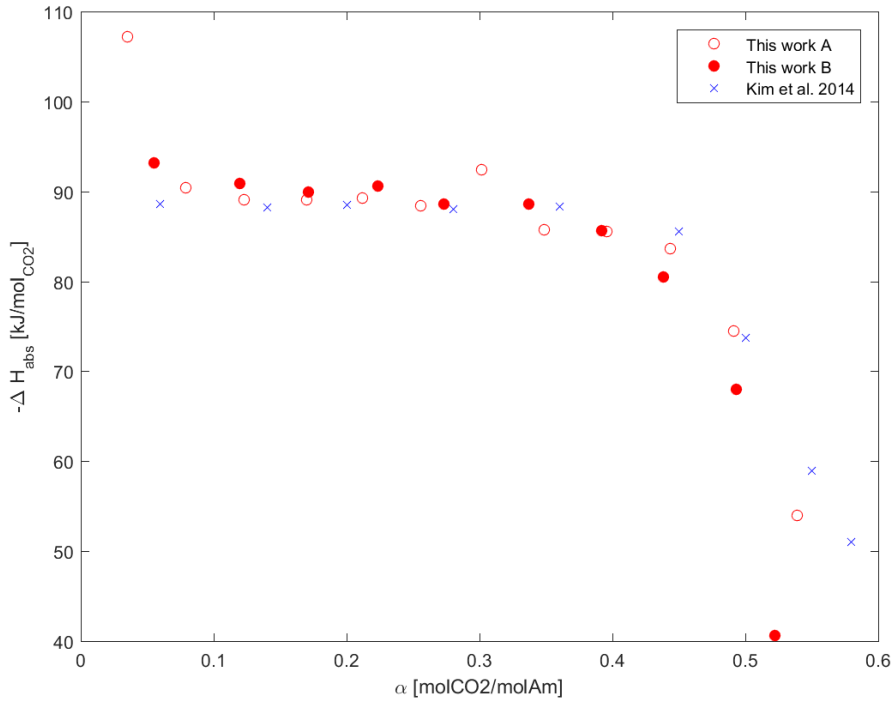

Figure 3.3: Measured heat of absorption in a 30wt% MEA solution at T= 80 °C. Experimental data from this work is compared to experimental data from previous work (Kim et al., 2014)

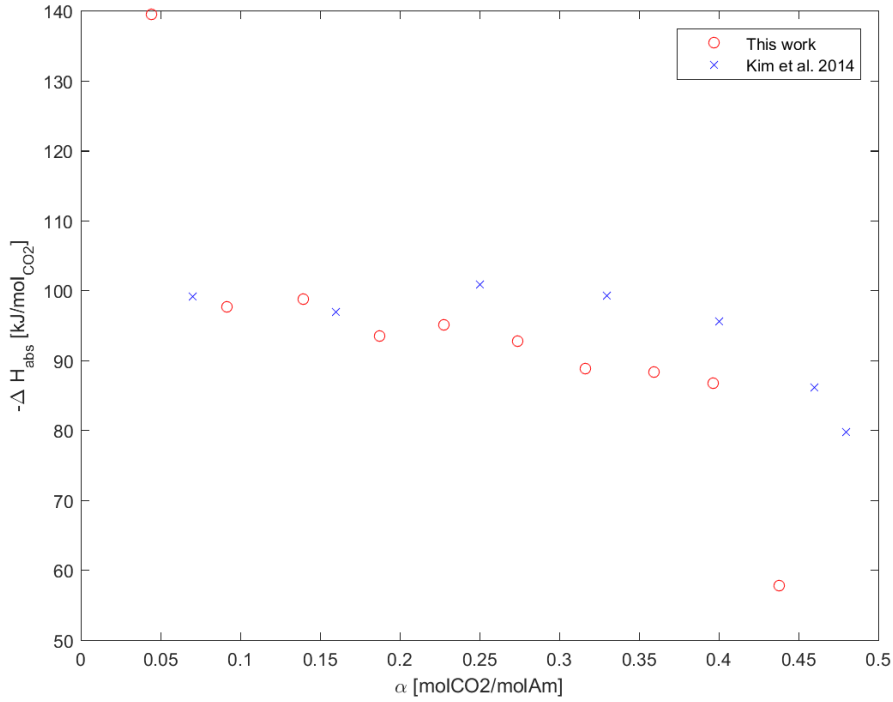

Figure 3.4: Measured heat of absorption in a 30wt% MEA solution at T=120 °C. Experimental data from this work is compared to experimental data from previous work (Kim et al., 2014)

absorption is almost constant at a value of 85 kJ/mol CO_2 up to a loading 0.4 mol CO_2/mol amine.

The results from this work also show good agreement with data from Kim at T=80°C. The heat of absorption is almost constant up to a loading around 0.5, before the values drop. At 120 °C the first point is very high, before the slope flattens out from a value around 100 kJ/mol CO_2 at loading 0.05 mol CO_2(mol amine)$^{-1}$. The results from this work show slightly lower values compared to the data from Kim. The differences might be explained by a difference in calibration or related to the integration-sequence of the total power. The latter will be further discussed in Section 3.1.1. There is a tendency of increasing start-values of the heat of absorption with increasing temperature. The same tendency is observed in the results from Kim and Arshad.

Generally the systems coincide well with data obtained by Kim and Arshad at T=40°C and T=80°C. The series at T=120°C fits well at the lowest

loadings, and then drops to lower heat of absorption than data from Kim. However, the differences are not considerable.

3.3 Heat of absorption: DEEA+MAPA

3.3.1 Verification of sample loading

The loading of the samples are analysed as described in section 2.3.4, and the sample is composed of known amounts of lean and loaded solution. The loading of the sample is calculated based on mass balance and weights. The amount of CO_2 is assumed to come from the loaded solution only, and the total moles of amines are the sum of moles of amines from unloaded and loaded solution. The analysed amounts of CO_2 and amines are reported as moles/weight of sample, and the analysed loading is found as the concentration of CO_2 divided by the concentration of amines. The concentration of CO_2 and amines in each sample are plotted in respectively Figure 3.5 and Figure 3.6.The sample loadings are presented in Figure 3.7.

The CO_2-concentrations - analysed and calculated from mass balance - in Figure 3.5 is generally well correlated although a few exceptions are evident. The values deviate from each other by ≈0-30%, where the analysed values are, in the majority of the samples, measured to be higher than the values calculated by mass balance. Possible sources of error in the CO_2-analysis are different concentrations of the titrant, loss of sample at transfer between bottles, uncertainty in the weight and uncertainty in pH-measurements.

Mass balance and analysed values of amine-concentrations are quite similar for MEA, 3D1.5M, 3D2M and 1D5M, with few exceptions. Note that some analysed values are removed due to strange results. The majority of the samples give analysed- and theoretical values deviate by less than 11%. The amine analysis are performed with small amounts of samples, ≈0.2g, which makes the analysis very sensitive for errors in weight and loss of sample. If the titrant is of high concentration there are small amounts of titrant needed to reach the equivalence point, which may lead to lower accuracy in the analysed values.

The final loadings of the samples, calculated from mass balance and analysed, are presented in Figure 3.7. Based on the deviations between analysed- and mass balance- values observed for both CO_2- and amine-concentrations described above, it is not surprising to see that there are occasionally large deviations between values of loading. The deviations between the two values

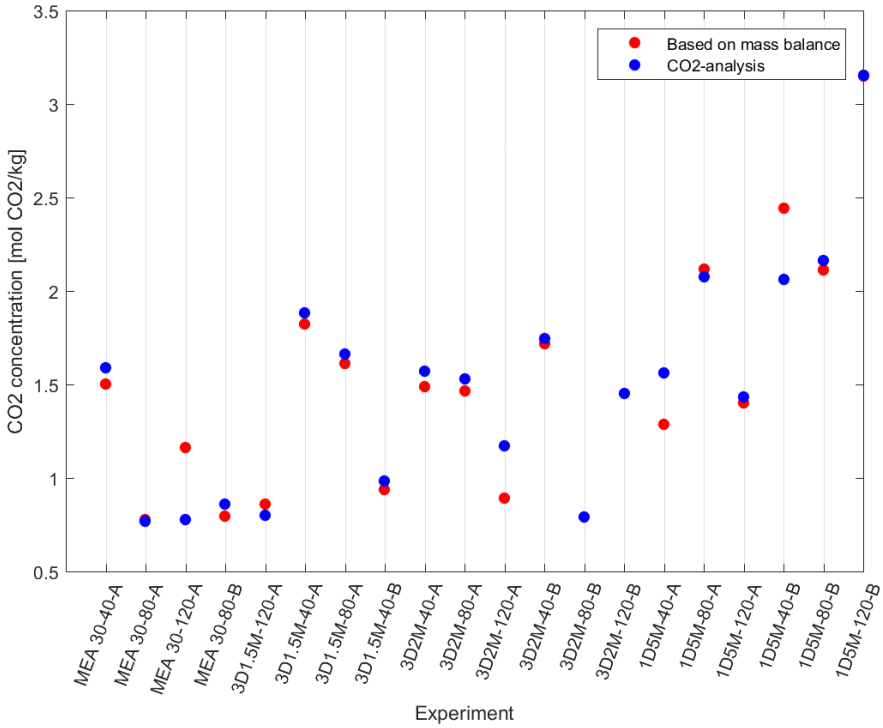

Figure 3.5: Concentration of CO_2 in sample. Concentration is calculated by mass balances and Peng-Robinson equation of state, and by titration analysis

are in the range of ±30%. The potential sources of error in each of the CO_2- and amine- analysis were discussed above. There are also potential errors related to insufficiently mixing, both in the reactor prior to sampling, and mixing of the sample bottles before execution of analysis.

The sampling has been challenging for some of the DEEA-MAPA blends. At 40 °C the final pressure in the reactor has been below atmospheric, which reduces the pressure difference between reactor and the sample cylinder. The viscosity of loaded DEEA-MAPA, especially at low temperature, is very high, and the flow out of the reactor was very or lacking. In some cases it was necessary to increase the reactor pressure by use of pressurized air to transfer loaded solution from the reactor to the sample cylinder. An increase in total pressure changes the original equilibrium loading, but due to the short time at higher pressure the effect is assumed to be small. The analysis were performed on all samples, but it was decided to exclude the results of 3D3M, 3D3.5M and 3.5D3.5M. The reason is that they form two phases,

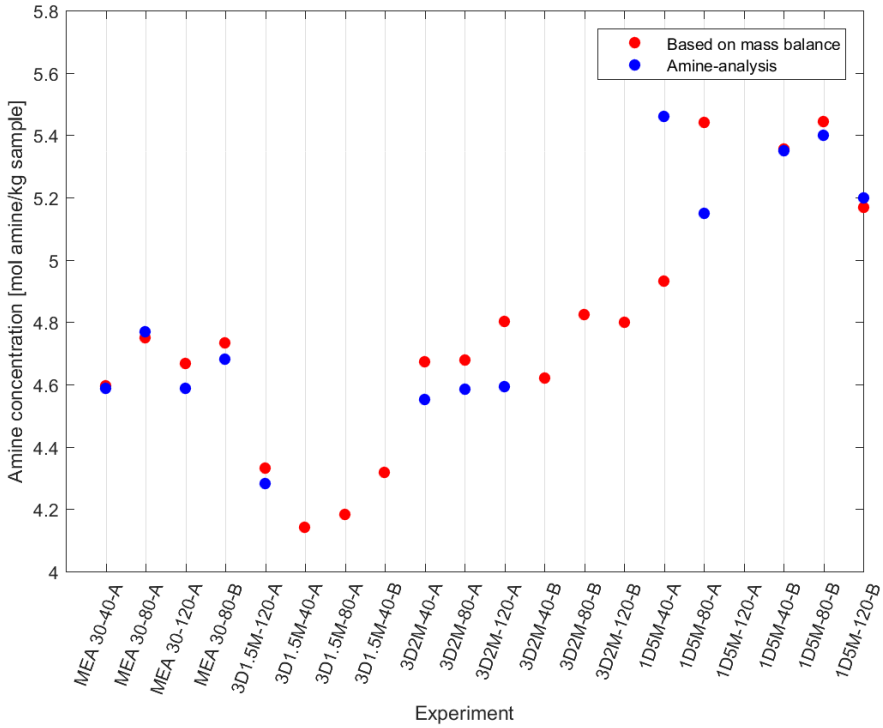

Figure 3.6: Concentration of amines in sample. Concentration is calculated by mass balances based on Peng-Robinson equation of state and by titration analysis

and there is no control on how much of each phase that is present in the sample. Some other amine analysis are also decided to be excluded, because they have values which deviate significantly from the values calculated from mass balance and are unlikely to be correct.

The sampling method and two-phase formation make this set of analysis less appropriate for determination of CO_2- and amine-concentration in DEEA-MAPA-systems. The degree of uncertainty related to the analysis and their results are significant, and should not be considered for verification of sample-loading calculated from mass balance.

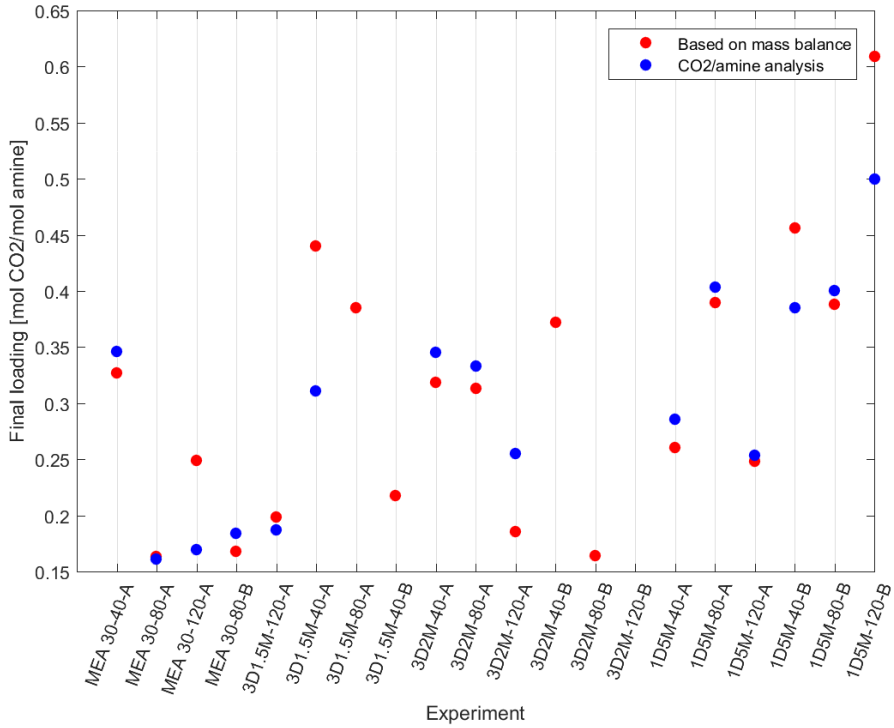

Figure 3.7: Loading of sample calculated by mass balances based on Peng-Robinson equation of state and by CO_2- and amine analysis

3.3.2 3M DEEA + 1.5M MAPA

Heat of absorption as a function of loading is presented in Figure 3.8 for all temperatures. Parallel 3D1.5M-80-A and 3D1.5M-120-B were discarded due to software crash during the experimental process. Due to time limitations they were not repeated. The two series at T=40°C follow each other closely, which indicates good reproducibility in this solution. The experiments performed at T=40° and T=80° have a relatively flat profile compared to the experiment at 120°.

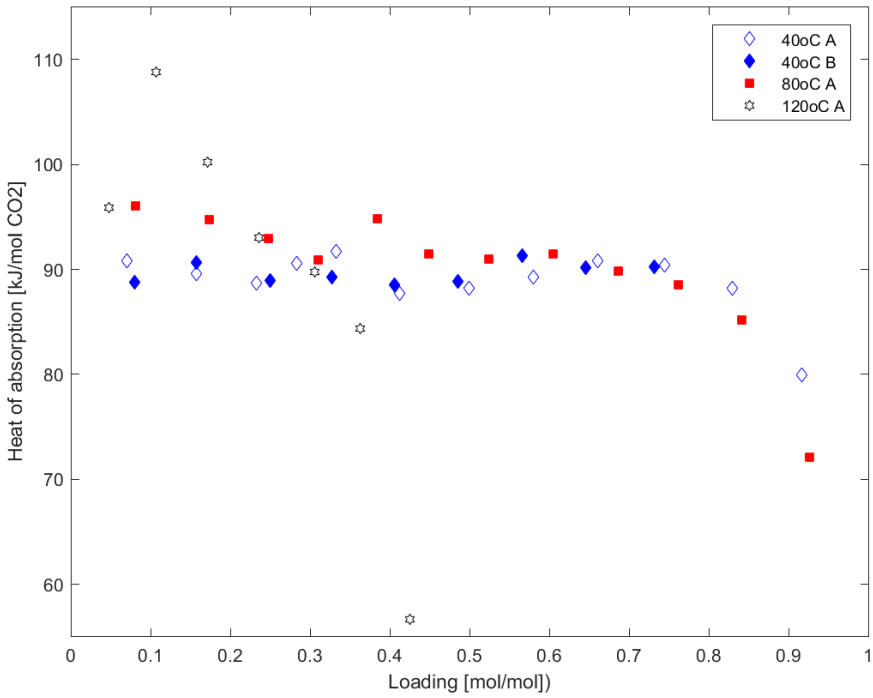

Figure 3.8: Plot of heat of absorption for CO_2 in a 3M DEEA+1.5M MAPA solution for temperatures 40, 80 and 120 °C.

3.3.3 3M DEEA + 2M MAPA

Heat of absorption as a function of loading for the 3M DEEA+ 2M MAPA solution is presented in Figure 3.9 for temperatures 40, 80 and 120 °C. A and B parallels shows well-correlated measurements and indicates trustworthy results for this system at all temperatures.

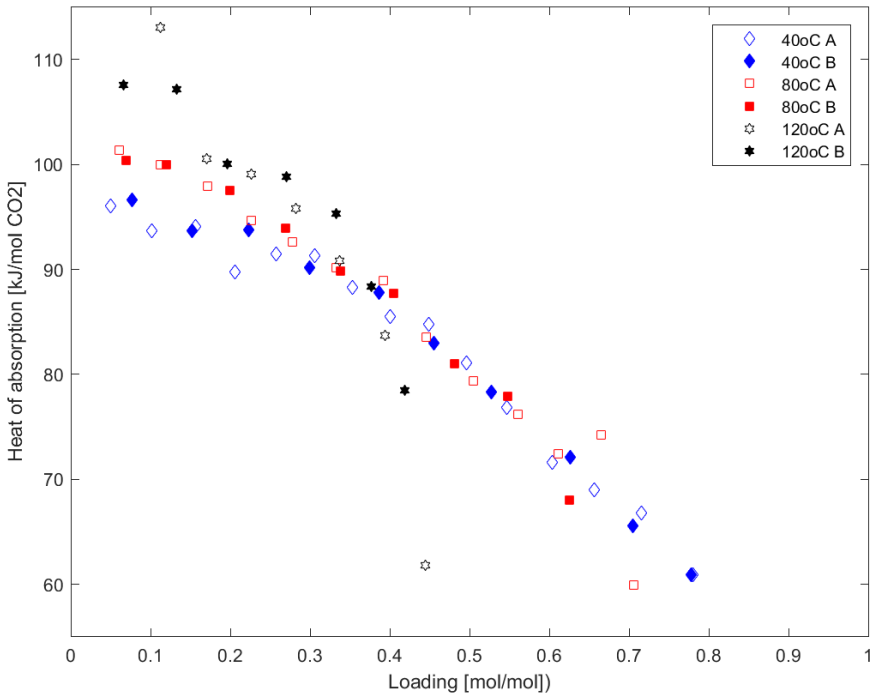

Figure 3.9: Plot of heat of absorption for CO_2 in a 3M DEEA+2M MAPA solution at 40, 80 and 120 °C.

3.3.4 1M DEEA + 5M MAPA

Heat of absorption as a function of loading for the experiments with solution 1D5M are given in Figure 3.10. One point in the 1D5M-120-B-experiment appears as an outlier (at loading ≈0.25), but there is nothing in the experimental process that may explain an erroneous at that point. The same is not observed in the A-parallel, and no other experiments have similar outliers. In this solution the relative differences between the three temperatures are smaller than what is observed in experiments of higher DEEA-concentration.

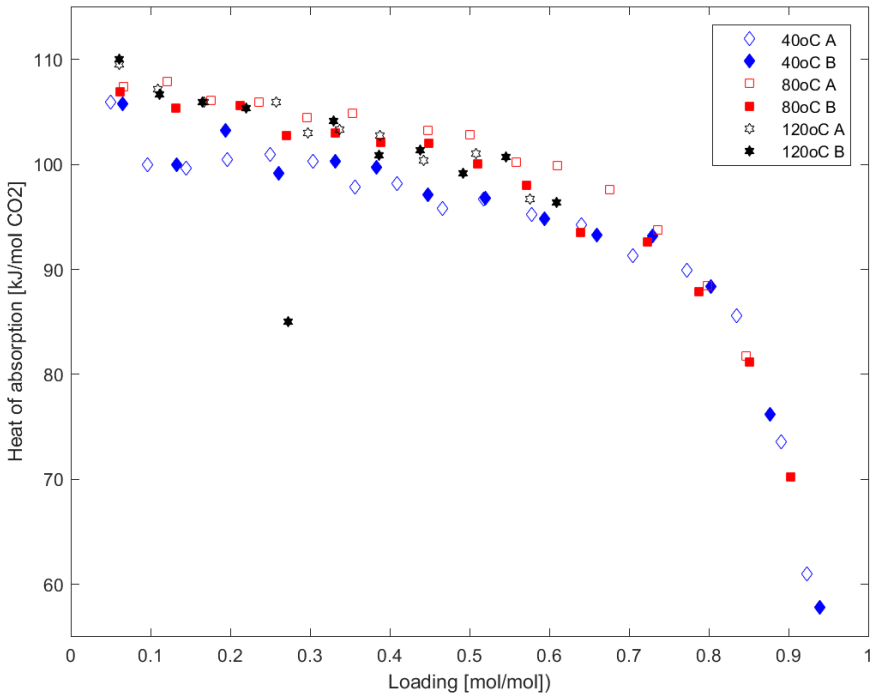

Figure 3.10: Plot of heat of absorption for CO_2 in a 1M DEEA+5M MAPA solution for temperatures 40, 80 and 120 °C.

3.3.5 3M DEEA + 3M MAPA

Heat of absorption as a function of loading for the 3D3M-solution is presented in Figure 3.11. The parallels at each temperature correlate well, indicating good reproducibility. The second loading in experiment 3D3M-120-B is a bit higher than the A-parallel, and is most likely a result of an experimental error.

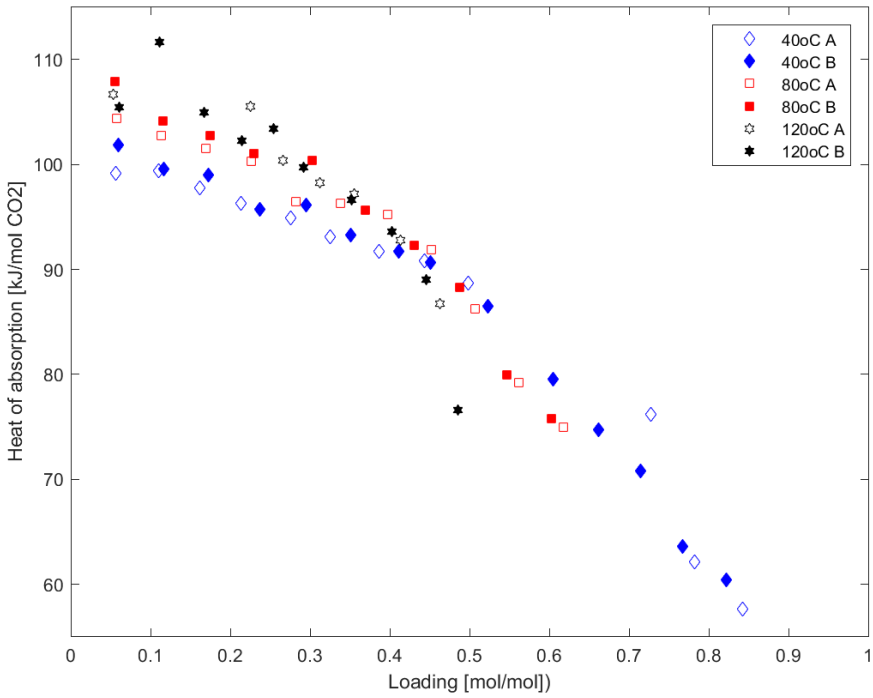

Figure 3.11: Plot of heat of absorption for CO_2 in a 3M DEEA+3M MAPA solution for temperatures 40, 80 and 120 °C.

3.3.6 3M DEEA + 3.5M MAPA

Heat of absorption per unit CO_2 as a function of loading is presented in Figure 3.12. During the 3D3.5M-120-A-experiment the pipeline leading CO_2 to the bottom of the reactor got partly clogged. The reason was most likely related to solution of high viscosity in the pipeline. The resulting effect was reduced CO_2-flow in each CO_2-loading during the experimental process, but as the system is completely sealed and allowed to reach equilibrium before integration of the total power it is assumed that the results are not corrupted. However, the values of the heat of absorption of the A parallel of 3D3.5M-120 drop off faster than the B-parallel, and the two parallels do not correlate as close as the other series. It is reasonable to assume that the clogging causes the deviation. Another possible cause is the use of different calorimeters, as the B-parallel was run in calorimeter 1. However, the 2 parallels at T=80°C are also run in two different calorimeters, but do not show the same degree of deviations. Calorimeter 1 was more sensitive to gas leakages, probably due to a worn gasket. Bolts needed to be tightened

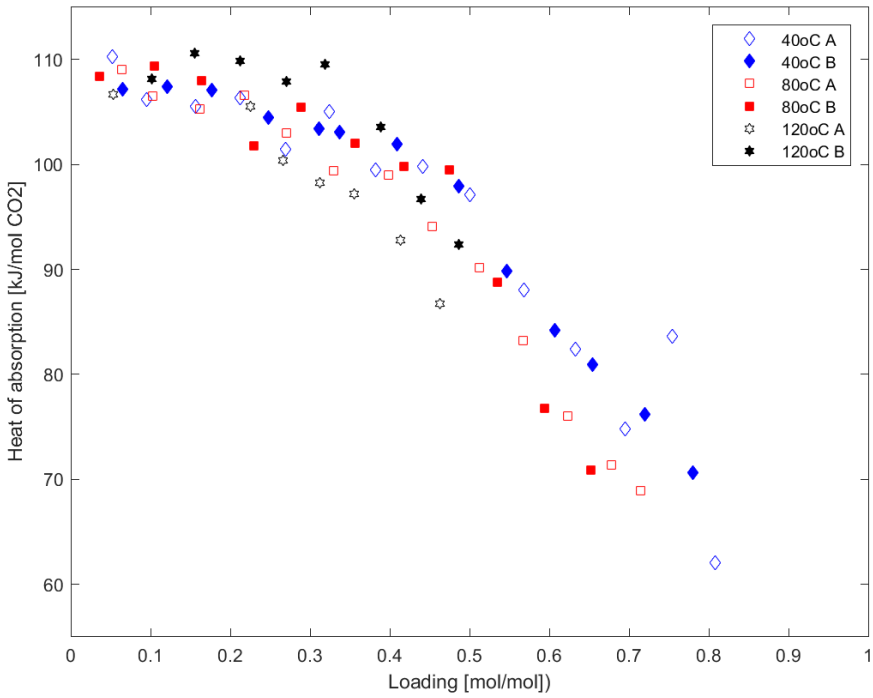

Figure 3.12: Plot of heat of absorption for CO_2 in a 3M DEEA+3.5M MAPA solution for temperatures 40, 80 and 120 °C.

hard to avoid leakages. This explains the unexpected increase in pressure that was observed in the first part of experiment 3D3.5M-40-B. The bolts were tightened and the experiment was continued. The heat of reaction of parallel A and B in 3D3.5M-40 correspond very well, thus, the pressure increase does not seem to affect the results significantly. This system shows a vague tendency of a having a lower slope up to a loading of $\approx$ 0.5 at T=40°C, before the heat of absorption values certainly drops. The trend is also visible at the other temperatures. This behaviour is more similar to pure MAPA- and pure DEEA-systems (Arshad, 2014)

An illustration of a loaded solution which has formed two phases is shown in Figure 3.13. The picture is taken approximately 24 hours after the final loading, at atmospheric pressure and a temperature of ~22°C. More pictures are attached in Appendix B.

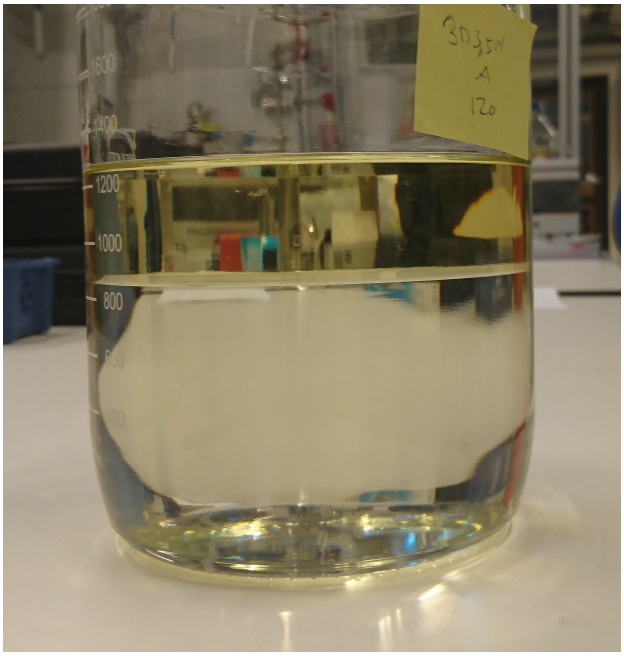

Figure 3.13: Illustration of a two-phase loaded solution. This picture is from experiment 3D3.5M-120-A, 1 day after the last loading, at T≈ 22°C and atmospheric pressure.

3.3.7 3.5M DEEA + 3.5M MAPA

Results from the one experiment with 3.5M DEEA and 3.5M MAPA is presented in Figure 3.14. The values of heat of absorption decrease very slowly up to a certain loading at ≈0.45 before it drops off fast. This is the same tendency that was observed in the 3D3.5M-system.

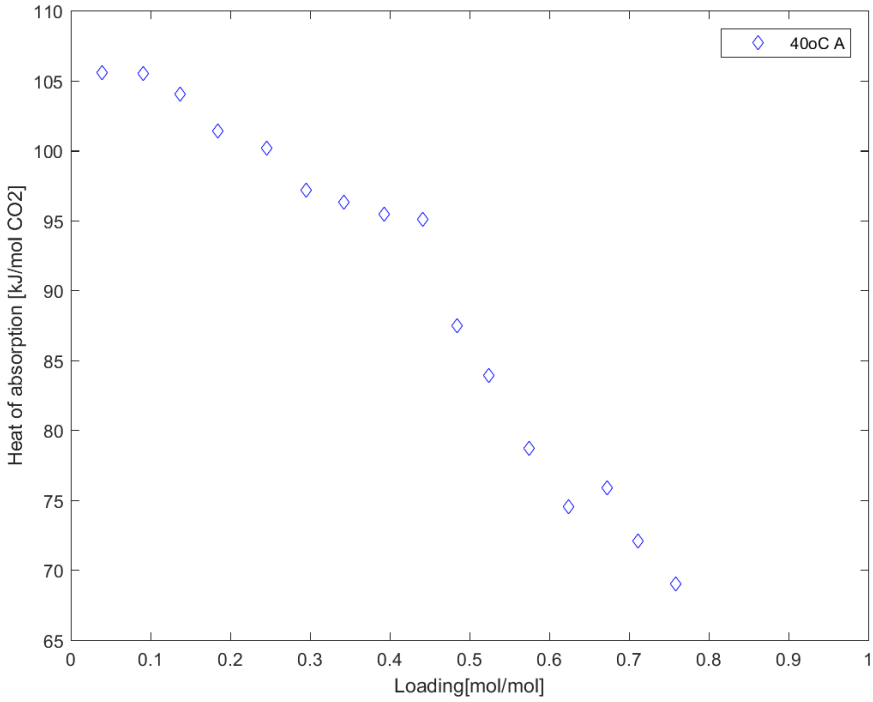

Figure 3.14: Plot of heat of absorption for CO_2 in a 3.5M DEEA+3.5M MAPA solution at 40 °C.

3.3.8 Temperature dependency in DEEA-MAPA systems

Experiments were terminated when a clear indication of maximum loading was established. As expected the slopes indicate a trend of decrease in maximum loading as the temperature increase, which corresponds to trends in data available in the literature (Kim et al., 2014) (Arshad, 2014) (Jonassen et al., 2014). For system 3D1.5M, 3D2M, 3D3M, 3.5D3.5M and 1D5M the values of heat of absorption during the first few loadings all show increasing proportionality to increase in temperature. In system 3D3.5M the values of heat of absorption at T=40°C and T=80°C correlates well, but series A and B at T=120°C have values which deviates considerably from the series at lower temperatures. This indicates that parallel A at T=120°C in 3D3.5M might be wrong.

In general. the difference in heat of absorption at the first few loadings (typically up to a loading of 0.3) between highest and lowest temperature

is typically ≈10% in the DEEA-MAPA blends, while the difference between the same temperatures series for MEA is slightly higher.

3.3.9 Concentration dependency in DEEA-MAPA-systems

Experiments performed at the same temperature (40, 80 and 120°C) are plotted together in Figure 3.15-Figure 3.17.

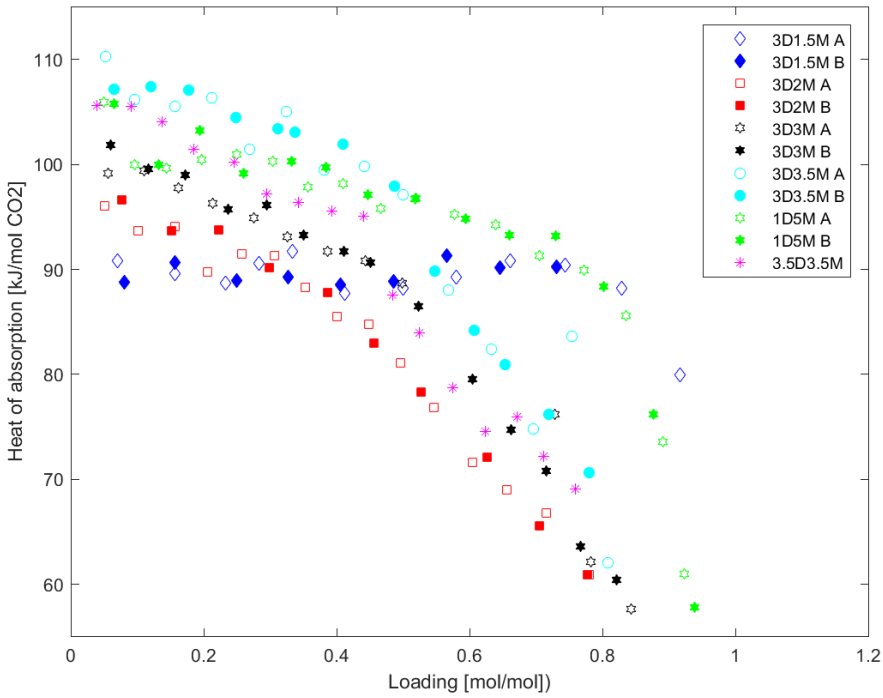

Figure 3.15: Heat of absorption as a function of loading for all experiments performed at 40°C

The MEA-system and systems with only one of the amines (MAPA-water and DEEA-water) studied by (Arshad, 2014), have nearly constant heat of absorption up to a relatively high loading. The blends of DEEA-MAPA have the highest value for heat of absorption at the first loadings, and continuously decrease as the loading increase. The exception is system 3D1.5M, which has almost constant values of heat of absorption up to a loading around 0.8 at T=40°C and T=80°C. This system has the lowest MAPA/DEEA-ratio of all blends studied in this work, and provides the lowest heat of absorption

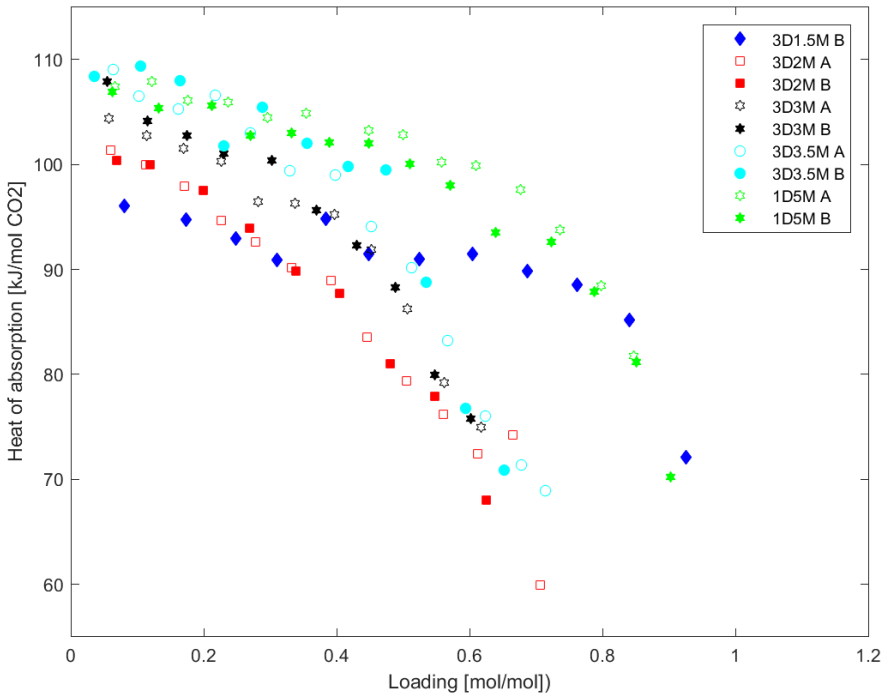

Figure 3.16: Heat of absorption as a function of loading for all experiments performed at 80°C

values for low loadings, at all temperatures. This may be explained by the lower heat of absorption in pure DEEA, which is the dominating compound, considering the concentration. DEEA-water-systems have lower heat of absorption than MAPA-water-systems, according to data from (Kim, 2014) and (Arshad, 2014).

System 1D5M has the highest MAPA-concentration of the experiments in this work, and the lowest concentration of DEEA. Even though the MAPA-concentration is highest, the measured heat of absorption is not the highest of the systems studied at any of the temperatures. The highest loading is achieved by the 1D5M-system, for all temperatures. It should be noted that the loading depends on the CO_2 partial pressure, which is not considered in this comparison, and the maximum achievable loading does not give a correct base for comparison of performance without studying VLE-data.

The systems may be compared by looking at the loading for each system at each specific value of heat of absorption. For instance, the heat of absorption value 80kJ/mol CO_2 at T=40°C in Figure 3.15 shows the 3D2M-system has

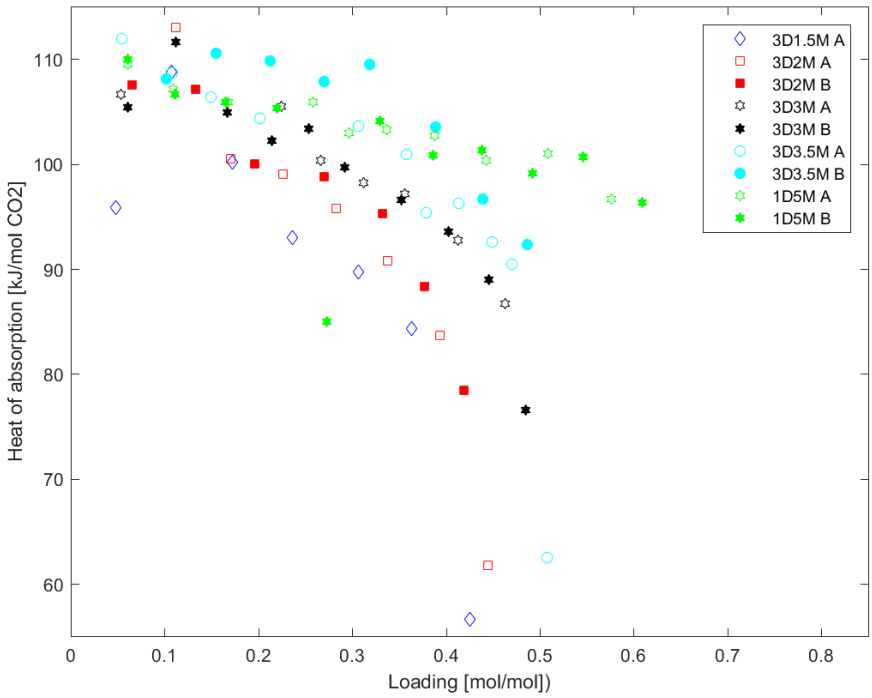

Figure 3.17: Heat of absorption as a function of loading for all experiments performed at 120°C

the lowest loading at ≈0.5, followed by 3D3M and 3.5D3.5M at loading ≈0.6, 3D3.5M at ≈0.7 and 1D5M and 3D1.5M at loading ≈0.9. At T=120°C in Figure 3.17 for a heat of absorption value of 95kJ/mol CO_2 the 3D1.5M-system has a loading of ≈0.05, followed by system 3D2M with ≈0.3, 3D3M at ≈ 0.4, 3D3.5M at ≈ 0.5 and 1D5M at≈ 0.65. The order is similar to what was found at T=40°C, except for system 3D1.5M which is one of the systems with highest loading at T=40°C, and the clearly lowest loading at T=120°C. A further discussion of the VLE at these specific loadings follows in Section 3.4.

System 3D1.5M stands out with respect to the heat of absorption values. As already mentioned, all systems have increasing values for heat of absorption at the lowest loadings as the temperature increases, but the difference between lowest and highest temperature at the first loading in the 3D1.5M-system is much smaller relative the other systems, with values around 90kJ/mol CO_2 at T=40°C and 95kJ/mol CO_2 at T=120°C.

There are three systems at T=80°C and T=120°C, and four systems at

T=40°C having a concentration of 3M DEEA (3M1.5M, 3M2M, 3M3.5M (3.5D3.5M)). There is a tendency of increasing start-values of heat of absorption at all temperatures with increasing concentration of MAPA. The loading decreases with increasing concentration of MAPA at T=40°C and T=80°C, but the trend is completely opposite at T=120°C.

3.3.10 Reaction of CO_2 with DEEA and MAPA

MAPA is recognized as a fast-reacting amine, while the tertiary amine DEEA has lower reaction rate (Monteiro et al., 2015). The difference in reactivity leads to the idea that all MAPA will react with CO_2 before DEEA get the chance to react. There is data available in literature for pure MAPA with concentration 2mole MAPA/kg(Arshad, 2014). The same MAPA-concentration is studied in the 3D2M-system in this work. Figure 3.18, Figure 3.19 and Figure 3.20 are plots of heat of absorption as a function of loading in respectively 3D2M-40, 3D2M-80 and 3D2M-120. Data for pure 2M MAPA at the same temperatures are plotted in the same figures. The vertical lines in the plots refer to a scenario where all added CO_2 reacts with only MAPA in the 3D2M-solution until the theoretical maximum loading of MAPA is reached (mol CO_2/mole MAPA= α_{MAPA}=1). The maximum loading is based on the assumption that both amine groups on the MAPA-molecule are reacted with CO_2. The line is the point where all MAPA is reacted.

The pure 2M MAPA at T=40° in Figure 3.18 has lower start values for heat of absorption than the 3D2M-solution, and shows a rather constant values up to a loading around 0.5. The 3D2M-solution starts out at higher values of heat for absorption at low loadings, and decreases steadily as the loading increases. At T=120°C the blend of 3M DEEA and 2M MAPA has a lower start values of heat of absorption than pure 2M MAPA, which indicates that a blend of the two amines gives more beneficial stripper conditions compared to pure 2M MAPA. The loading of the 3D2M is presented as mole CO_2 per *total* moles amine in the blend, not only the 2M MAPA in the blend. Thus, the units on the x-axis do not allow for direct comparison on the pure 2M-MAPA and the 2M-MAPA in the blend. However, a flat shape of the 3D2M-graph at the same values of heat of absorption would have been expected if MAPA reacts faster. Such a trend is not observed here. The same trends of constant heat of absorption values for pure MAPA and steady decreasing values in the 3D2M-blends are found at T=80°C and T=120°C in Figure 3.19 and Figure 3.20.

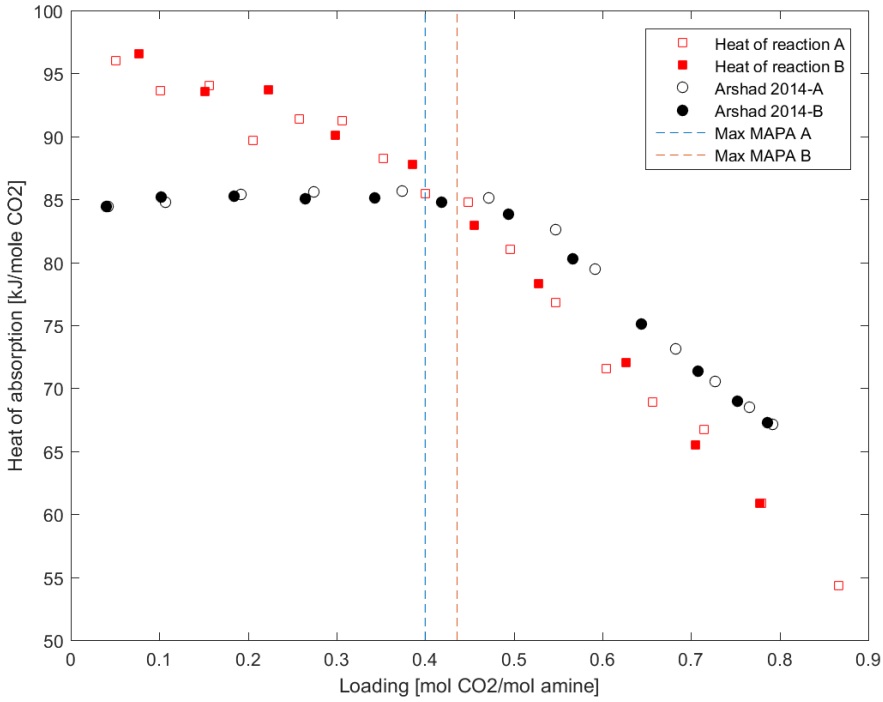

Figure 3.18: Heat of absorption as a function of loading in 3D2M-40. The vertical lines indicate the point where all MAPA is reacted with the CO_2 added to the system, if only MAPA was allowed to react.

The differences in heat of absorption between pure 2M MAPA at different temperatures are relatively large. The blend with highest concentration of MAPA in this work, 1D5M, shows very *small* differences between the temperatures, presented in section 3.3.4. This supports the theory that DEEA is affecting the absorption, even at low loadings.

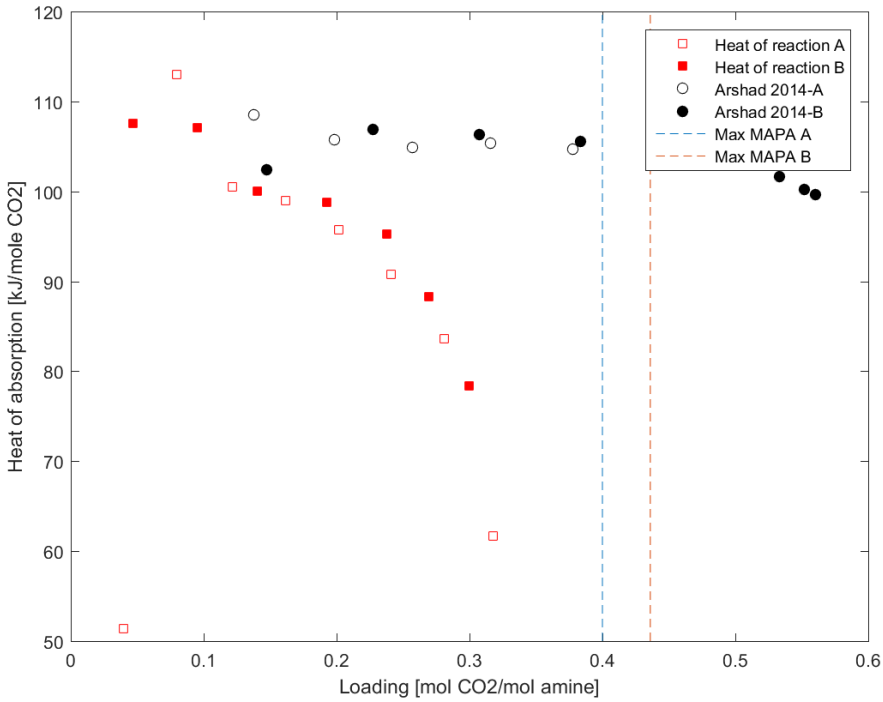

Figure 3.19: Heat of absorption as a function of loading in 3D2M-80. The vertical lines indicate the point where all MAPA is reacted with the CO_2 added to the system, if only MAPA was allowed to react.

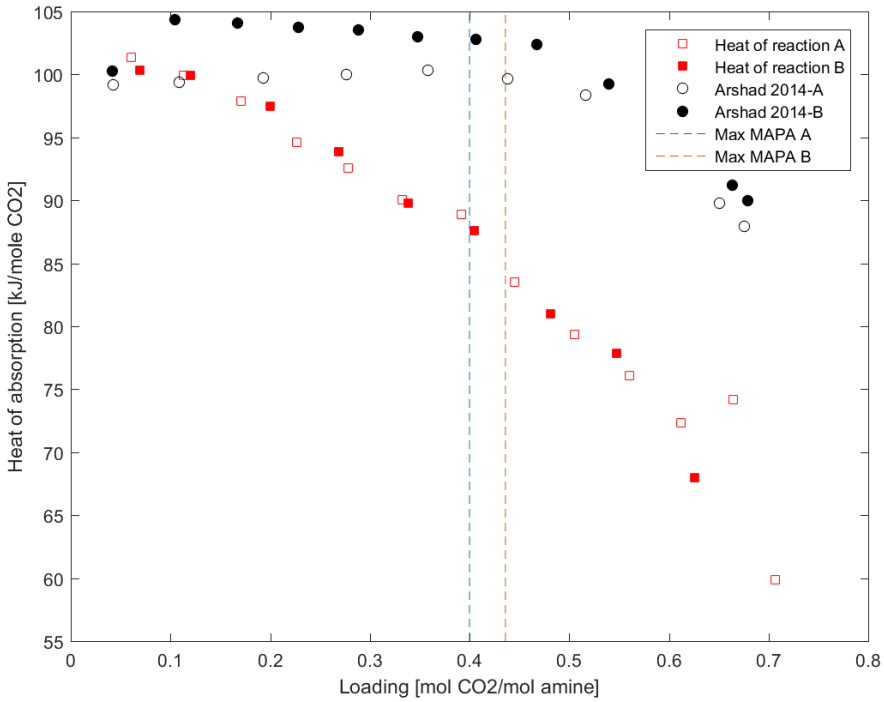

Figure 3.20: Heat of absorption as a function of loading in 3D2M-120. The vertical lines indicate the point where all MAPA is reacted with the CO_2 added to the system, if only MAPA was allowed to react.

3.3.11 Colours

The observed colours of lean and loaded solutions are presented in Table 3.2. All observations are done minimum 24 hours after the end of the experiment, such that the temperature is ≈22°C. Pictures of some of the loaded solutions are included in Appendix B.

DEEA is bought in 2L-bottles, whereas the colour of the content varied for different bottles. The colours of pure DEEA was either blank or yellow. The colour of the DEEA also became the colour of mixed solutions of DEEA and MAPA. Thus, two similar blends of DEEA-MAPA could have different colours of unloaded solution. The MSDS for DEEA included in Appendix C reports that DEEA in pure form is a clear, colourless fluid. However, the results from heat of absorption measurements do not show any indications of different behaviour for similar systems of different unloaded colour.

Some interesting observations are made on the loaded solutions. For some concentrations the loaded solutions of similar blends, performed at the same temperature, turn out to have different colours at final loading. One example is the 3D1.5M at 40°C, where both A and B start out as a blank solution and end up as respectively blank and pink. The same solutions at higher temperatures are all colourless. The 3D2M- and 1D5M-solutions are pink at 40°C, lighter pink at 80°C and blank at 120°C. The results indicates that higher temperatures lead to less colour. As the temperature increase the final loading decreases, which could imply that the solutions are more pink at high loadings, and lower loadings are colourless. The yellow A-parallel of 3D2M ends up with pink colour at 40°C, and are blank for the execution at 80 and 120°C. The B-parallel of solution 1D5M is pink at the final loading at 40°C, but ends up as yellow at 80°C and °C. In the 3D3.5M-experiments there are actually two parallels which show the same trend in colour, going from pink at 40°C, and slightly yellow at 80 and 120 °C.

Solutions 3D3M, 3D3.5M and 3.5D3.5M were all run to relatively high loadings at atmospheric pressure in the experiments for observations of two-phase formation reported in Section 3.5. These solutions were blank when unloaded, and never changed colours at any loadings, other than becoming opaque and sticky. There are no clear trends observed in change of colours as a function of concentrations and temperatures in the solutions. However, many of the solutions support the tendency of darkest colour at execution at lowest temperature, and show a decreasing saturation of colours as the temperature increase. As mentioned above, one explanation of different colours is the difference in loading, indicating more saturated colours at high

loading, and decreasing saturation as the loading decreases. Another explanation may be degradation of the amines, which will probably be higher with execution at higher temperatures. However, degradation is not very likely within the short time period of one experiment, and strong degradation does normally give coloured solutions.

3.4 Vapour-Liquid-Equilibrium (VLE)

Calculation procedure for VLE-data is described in Section 2.5.3. As mentioned, VLE-data is based on the assumption that all change in total pressure is due to change in partial pressure of CO_2. The assumption implies that the vapour pressure of the amines-water solution is independent of CO_2-loading. In the majority of the experiments it was observed a small *decrease* in total pressure at the two-three first loadings. This indicates a decrease in vapour pressure of the amine solution, and contradicts the assumption of the amine solution vapour pressure being independent of loading.

In conversation with (Rennemo, 2015a) he stated that the same decrease in total pressure was observed in his experiments. The decrease in total pressure was most significant at 40°C, and in the systems with highest DEEA-concentrations. The decrease in total pressure is relatively small, typically a reduction of 0.001-0.015bar. As VLE-measurements were not the main focus in this work the significance of the change in vapour pressure is assumed to be negligible in presentation of the data.

The only blend which is studied both in this work and by others regarding VLE is the 1M DEEA+5M MAPA. VLE-data from Rennemo (Rennemo, 2015b) is used for comparison with the 1D5M-solution in this work at temperatures 40°C, 80°C and 120 °C, see Figure 3.21-Figure 3.23.

VLE-data from system 1D5M in Figure 3.21-Figure 3.23 show good correlation with data from Rennemo at all temperatures, with the exception of parallel B at 40°C. This observation supports the assumption of negligible effect from the change in amine vapour pressure as a function of loading.

VLE-data is essential in prediction of the behaviour of a CO_2-absorption/desorption process. (Farzad, 2014) has modelled a calorimeter using a rigorous thermodynamic model and the eNRTL-model to predict the results. The model was build for absorption of CO_2 in 30wt% MEA. The goal of the work was to use measured data directly in thermodynamic modelling and avoid assumptions related to, for instance, vapour pressure of water and amine. The VLE-data,

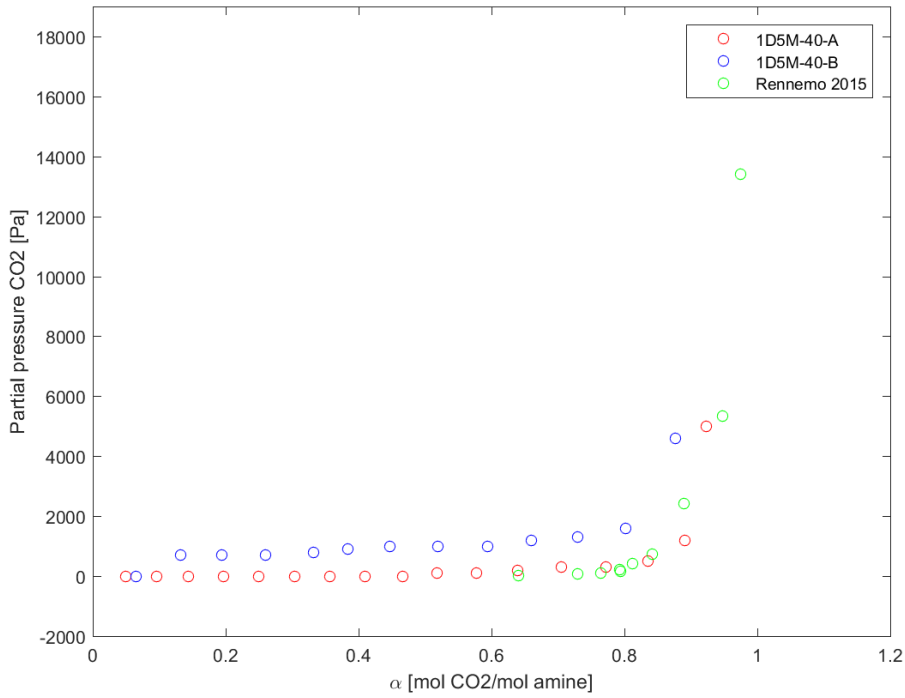

Figure 3.21: VLE as a function of loading at T=40 °C for system 1D5M

as well as the heat of absorption data from this work, could potentially be used for fitting of an equilibrium model for DEEA-MAPA, as preliminary investigated by Farzad for the MEA-system. However, calculating the CO_2 partial pressure from changes in total pressure is very sensitive to errors, as the amount of CO_2 in the gas phase is very small compared to the total pressure.

All VLE-data, including the data discussed above, is presented in Figure 3.24, Figure 3.25 and Figure 3.26. The figures include data for experiments performed at temperatures 40°C, 80°C and 120°C, respectively.

A leakage in the reactor occurred during experiment 3D3.5-40-B, as mentioned in Section 3.3.6, and VLE-data for this experiment is discarded. Data graphs for all systems is presented as a function of loading of CO_2 per mole of amine*groups* is included in Appendix B.3. To avoid confusion, loading as mole CO_2 per amine groups is hereby referred to as *amine-group-loading*.

Figure 3.24 allows for comparison of VLE for all the systems containing 3M DEEA at T=40°C. The partial pressure of CO_2 is increasing for increas-

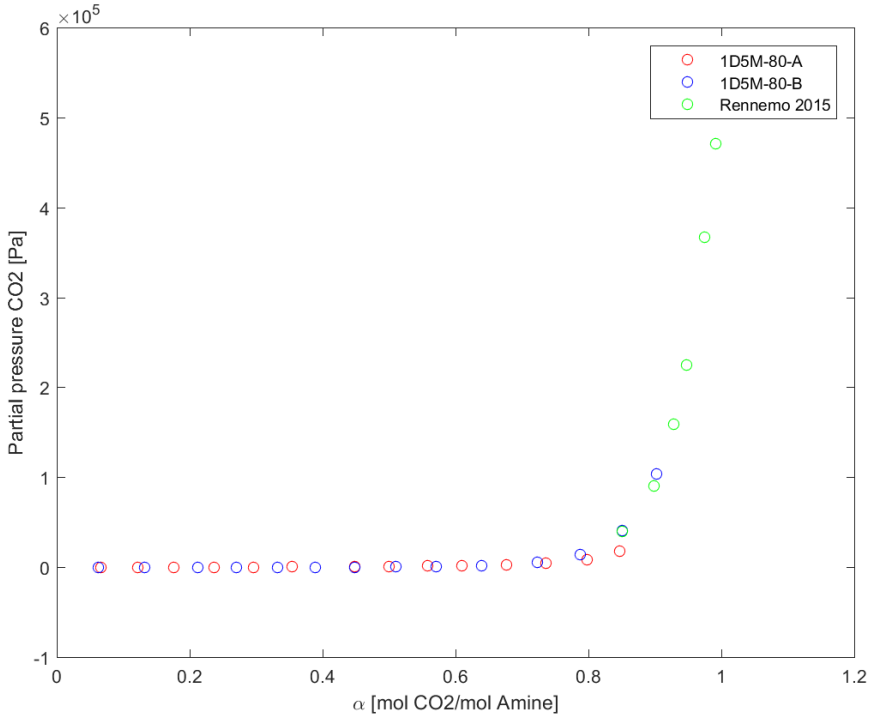

Figure 3.22: VLE as a function of loading at T=80 °C for system 1D5M

ing concentration of MAPA at the same loading. At 40°C the 3D1.5M- and 1D5M-systems reach a loading of ≈1, and still have a relatively low partial pressure of CO_2 compared to the other systems. Figure B.12 in Appendix B.3 shows partial pressure of CO_2 as a function of amine-group-loading at 40°C. The figure shows that the partial pressure of CO_2 starts to increase at an amine-group-loading of ≈0.38 in all the systems. The rate of the increase differ. The steepest rate is observed for the 3.5D3.5M-system, and lowest rate is observed for the 3D1.5M-system. The 1D5M-system, which had a relatively low gradient when presented as a function of loading in Figure 3.24, appears to have a rather steep increase in partial pressure as a function of amine-groups-loading.

Figure 3.25 show VLE-data at 80°C. The loading at where the partial pressures starts to increase significantly for all the systems is lower compared to T=40°C, around 0.3, while it happened around 0.6 at T=40°C. The 4 systems with 3M DEEA which showed a trend of increasing partial pressure for increasing concentration of MAPA at 40° does *not* show the same trend at 80°. The 3D1.5M-system is still the one with lowest partial pres-

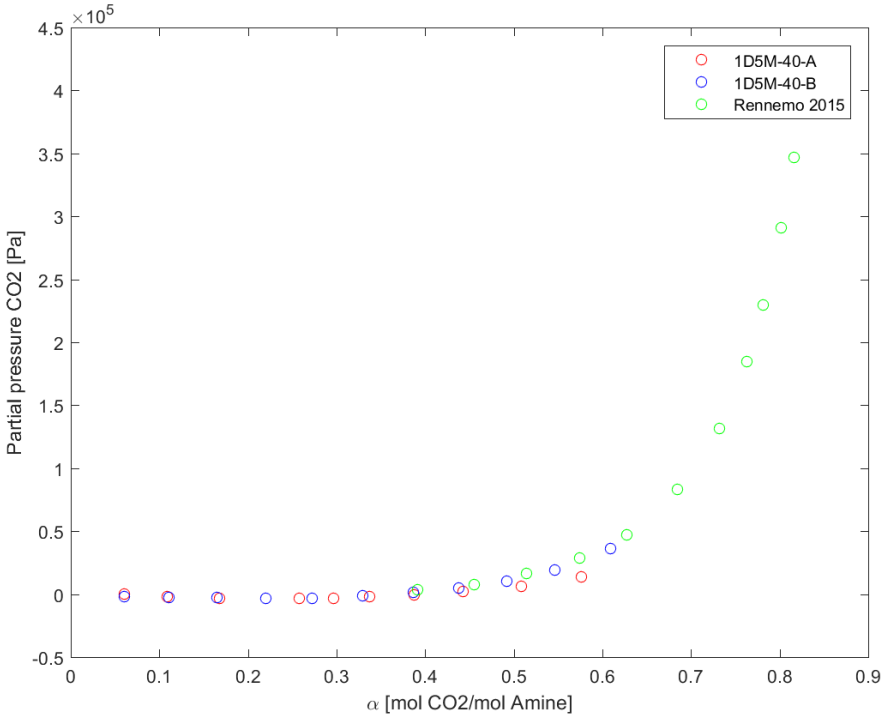

Figure 3.23: VLE as a function of loading at T=120 °C for system 1D5M

sure at highest loading, but all the other systems follow each other more closely at T=40°C. The 1D5M-system reaches a loading close to 1, and at this loading the partial pressure is quite low. At T=120°C in Figure 3.26 the trend for the systems with 3M DEEA is completely opposite from what was found at T=40°C. At loading 0.4 the 3D1.5M has the highest CO_2 partial pressure, while system 3D3.5M has the lowest, indicating an increasing partial pressure with increasing concentration of MAPA. System 1D5M is the system with lowest partial pressure at this loading. Regarding an absorption/desorption process it is preferable to have a system with low CO_2 partial pressure at low loading at low temperature, and high CO_2 partial pressure at high temperature, which will enhance the stripping process.

System 1D5M has relatively low partial pressure at all temperatures. The low partial pressure at T=40°C makes the system attractive as an absorbent, but the low partial pressure at T=120°C indicating poor stripping performance. 3D1.5M has the desired properties regarding VLE, with the lowest partial pressures at T=40°C and the highest at T=120°C.

At a higher temperature the same loadings correspond to higher CO_2 par-

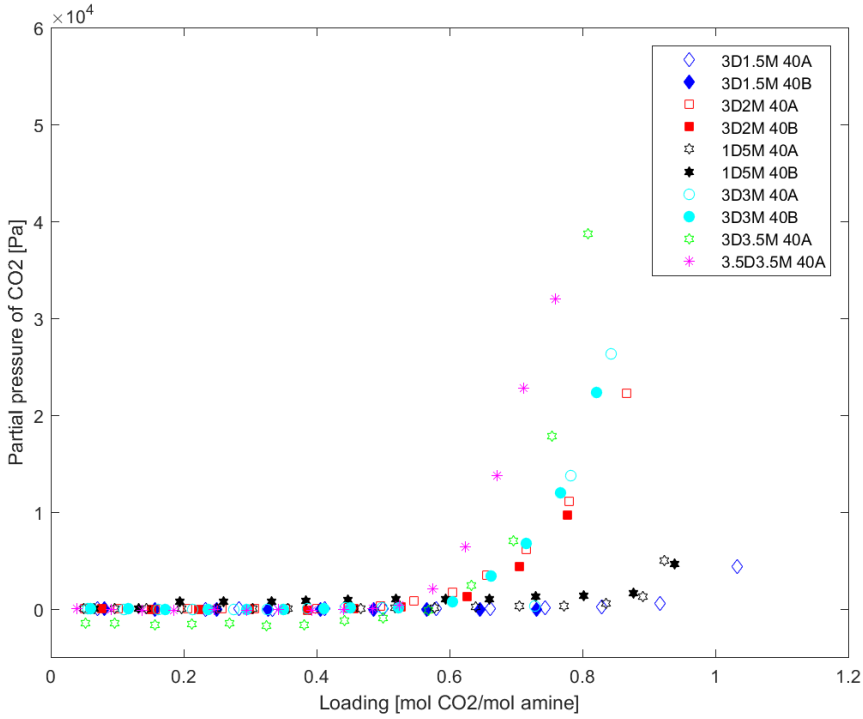

Figure 3.24: VLE-data from this work for all experiments performed at T=40°C.

tial pressure. For instance, system 3D2M at loading 0.4 takes CO_2 partial pressure values of approximately 0.01bar, 0.4bar and 1bar at temperatures T=40°C, T=80°C and T=120°C, respectively. This is consistent with VLE-data in literature from other amine systems(Kim, 2009).

In Section 3.3.9 the loadings at specific values for heat of absorption were compared for the different blends at T=40°C and T=120°C. At heat of absorption values 80kJ/mol CO_2 and 95kJ/mol CO_2 at respectively T=40°C and T=120°C, the 3D1.5M system has loaded values 0.9 and 0.05. The CO_2 partial pressures at loading 0.05 at T=120°C is close to 0bar, and the CO_2 partial pressure at loading 0.9 at T=40°C is 0.043bar, which is the lowest of all systems at this loading. Of all systems studied the 3D1.5M shows the most favourable properties with respect to heat of absorption values and VLE at absorption- and desorption temperatures.

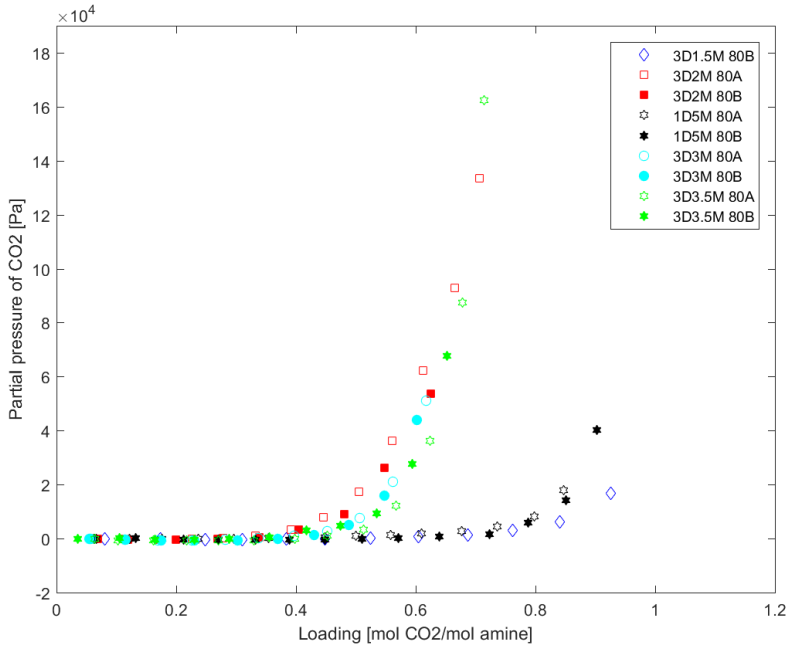

Figure 3.25: VLE-data for all experiments performed at T=80°C.

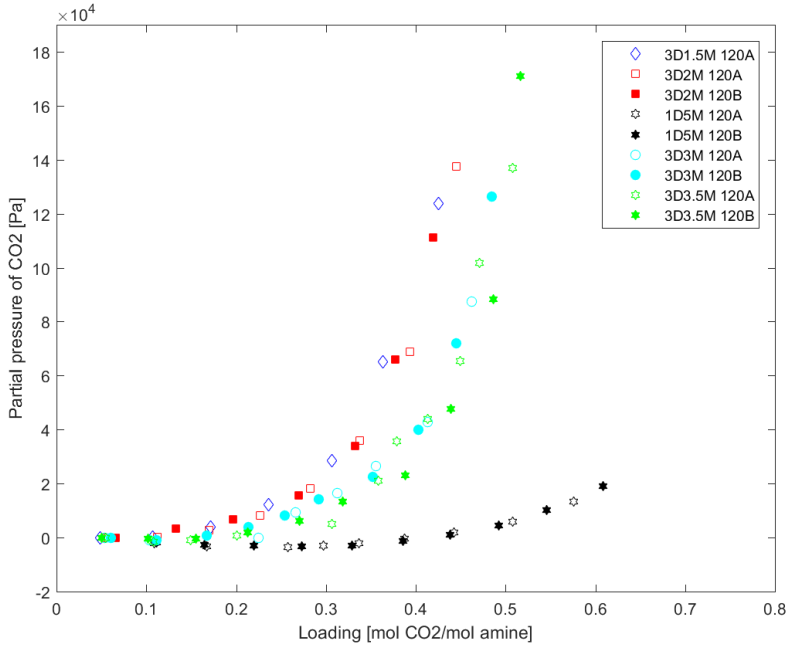

Figure 3.26: VLE-data for all experiments performed at T=120°C.

3.5 Observations of two-phase formation

Two-phase formation studies were performed for the 3D3M, 3.5M3.5M and 3D3.5M solutions in a glass cylinder. The temperature- and pressure conditions in these experiments are different from the conditions in the reactor calorimeter, and the experiments were performed as a simple visualization of the two-phase-formation. A picture from the 3D3.5M-experiment is shown in Figure 3.27.

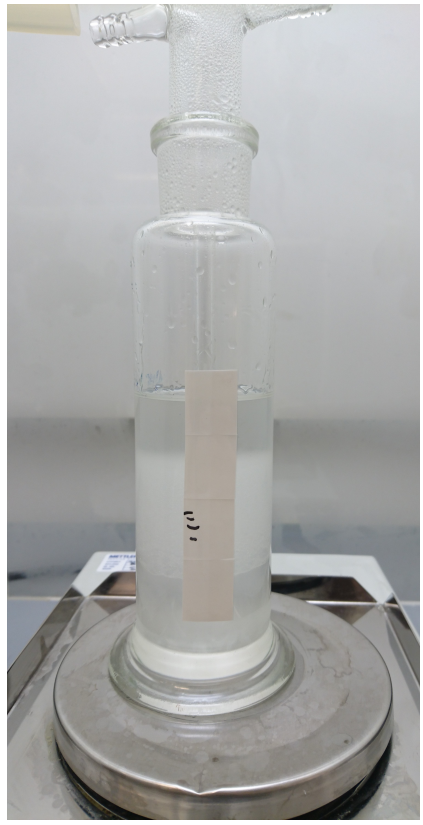

Figure 3.27: A picture from the two-phase formation experiment, here represented by the 3.5D3.5M-experiment

The height of the lower phase relative the total height for all the experiments are plotted in Figure 3.28. Two-phase formation occur at loadings of about 0.3, and increases for increasing loading for all the experiments. Around a loading of 0.55 the 3D3.5M solution becomes an one-phase solution. The same happens for system 3.5D3.5M and 3D3M at a loading of $\approx$0.65 and $\approx$0.7, respectively. The 3.5D3.5M-solution has the largest variations in height of the lower phase, ranging from around 0.45 to 0.9. Sys-

tems 3D3M and 3D3.5M have the lowest relative height of the lower phase of ≈0.65.

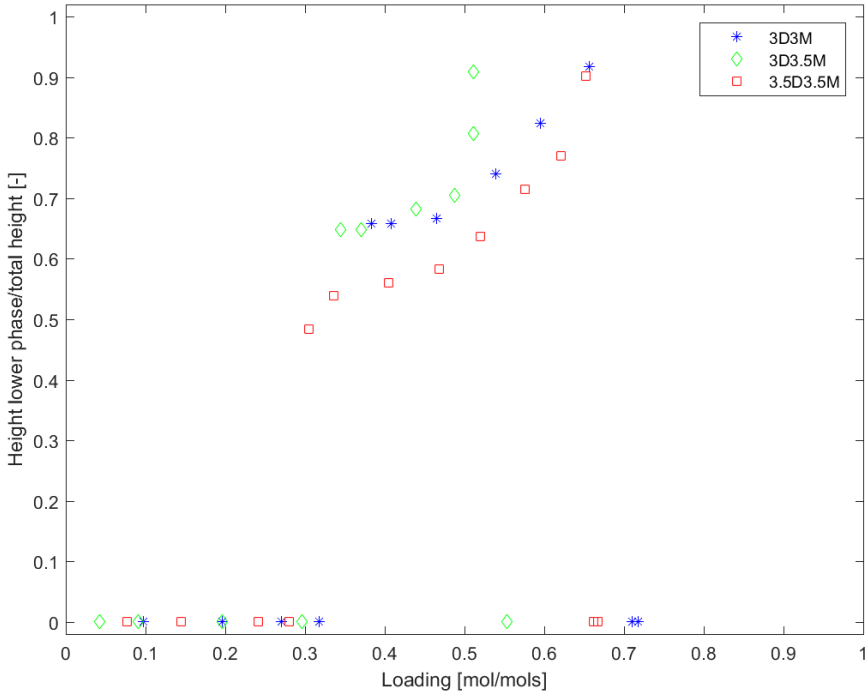

Figure 3.28: The height of the lower phase relative the total height as a function of loading for solutions 3D3M, 3D3.5M and 3.5D3.5M.

3.5.1 Heat of formation and two-phase formation

Figure 3.29 to 3.31 show the lower and upper limit with respect to loading where two-phase formations are observed for solution 3D3M, 3D3.5M and 3.5D3.5M. The same figures also include results from the heat of absorption experiments for the respective solutions at 40°C. The temperature 40°C was chosen because it is closest to the temperature in the cylinder where the two-phase-observations are made.

The two-phase formation experiments are performed in an open system, thus implying that the pressure is atmospheric and that the temperature varies as heat is released from the reaction. Indeed, several assumptions are made. If the two-phase formation is independent of temperature, there is no clear indication that the two-phase has a considerable impact on the values of

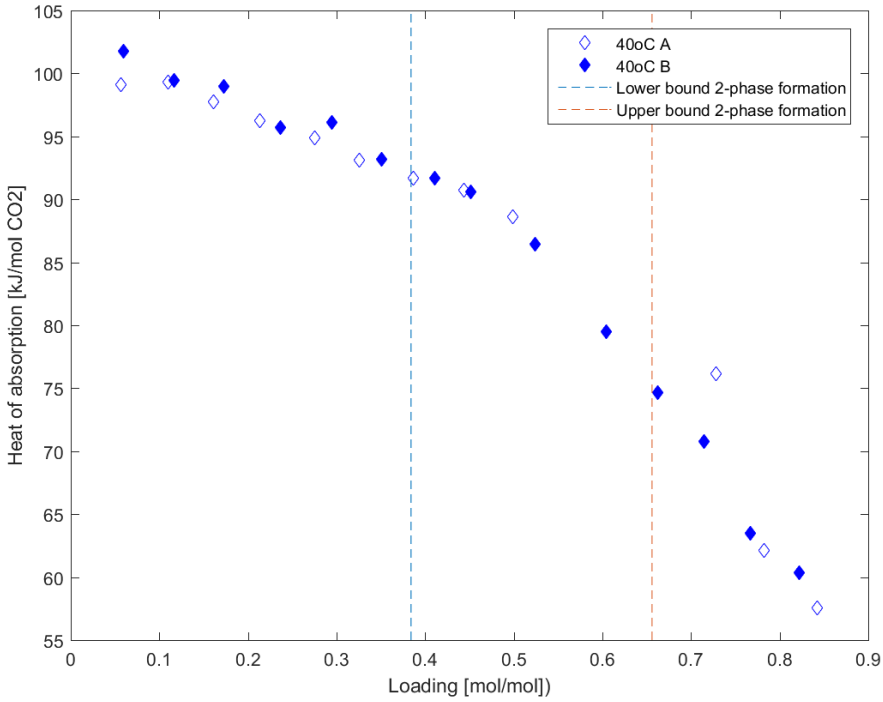

Figure 3.29: The lower and upper loading limits for two- phase formation observed for solution 3D3M. The figure also include the results from heat of absorption experiments for the respective solutions at 40 °.

heat of absorption. There are no clear increase or drop in heat of absorption values. The only vague indication is for the 3D3.5M in Figure 3.30, where a has a small drop is observed at the two-phase to single phase transition.

The 3D3M-solution has also been studied by Ida Bernhardsen (Bernhardsen, 2015). In conversation with Bernhardsen she reports that two phases occurred at loading 0.3409, with a maximum loading of 0.945. Two phases are first observed in the experiment in this work is at loading 0.38. This value is slightly higher than the loading observed by Bernhardsen, but the two observations indicates good correlation. A proposal for future VLE-experiments would be to increase the frequency of the loadings, thus increasing the accuracy.

Solution 3D3M and 3D3.5M were loaded directly to a loading where two phases are present in a separate experiment. The height of the lower phase relative the total height of the solution is presented in Table 3.3 at two temperatures. The purpose is to study the temperature dependency of the

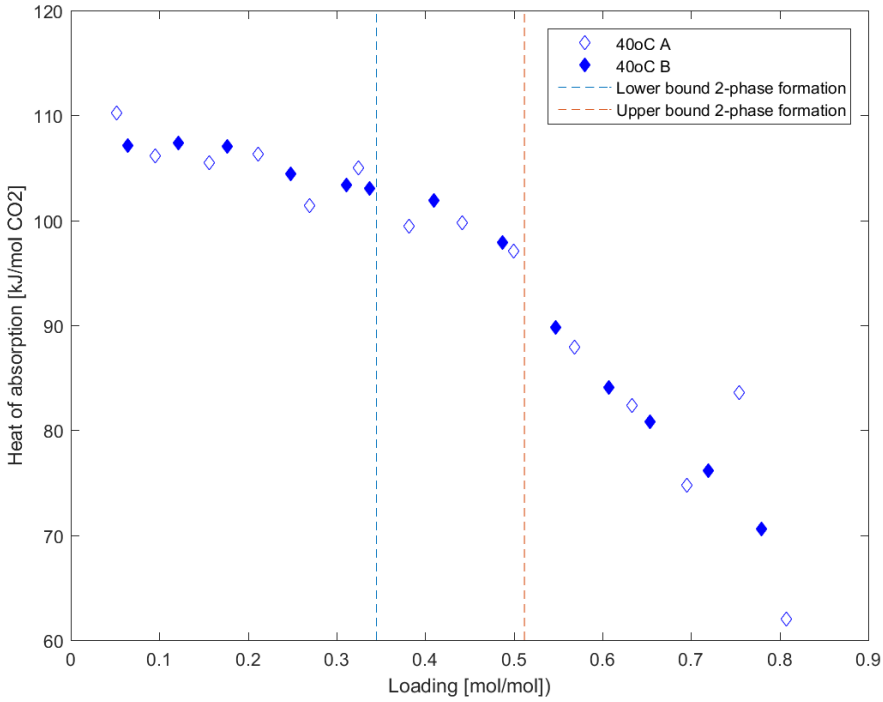

Figure 3.30: The lower and upper loading limits for two- phase formation observed for solution 3D3.5M. The figure also include the results from heat of absorption experiments for the respective solutions at 40 °.

height of the phases.

Table 3.3: The height of lower phase relative the total height at two temperatures for solution 3D3M and 3D3.5M.

Solution	$\approx 22°C$	**50°C**
3D3M	0.636	0.627
3D3.5M	0.655	0.651

Table 3.3 shows that the difference in the height of the lower phase relative the total height do not differ significantly between T=22°C and T=50°C. The two solutions indicates a weak tendency of larger lower phase fraction T=22°C, but the difference is small, and might be a result of error in measurements. There is a possibility that the temperature dependency is more significant at higher temperatures, and between larger temperature differences. However, the small differences of the phases between T=22°C and

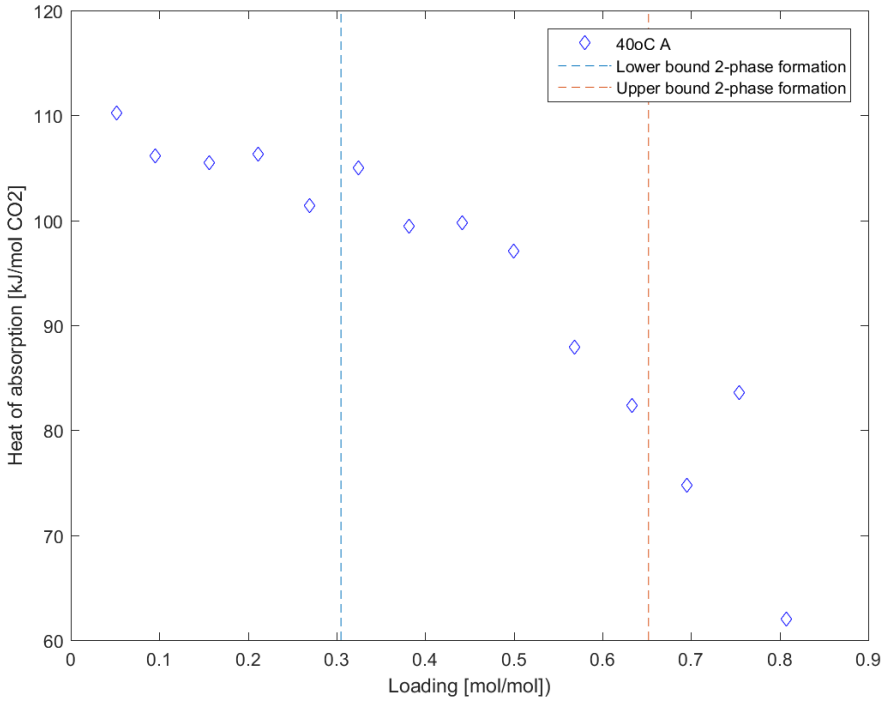

Figure 3.31: The lower and upper loading limits for two- phase formation observed for solution 3.5D3.5M. The figure also include the results from heat of absorption experiments for the respective solutions at 40 °.

T=50°C support the theory that the results from two-phase observations can be used for comparison to heat of absorption values.

3.5.2 VLE and two-phase formation

VLE-data for the systems known to form two phases are plotted in Figure 3.32 at T=40°C. T=40°C is chosen for comparison as it is the temperature closest to the temperature in the two-phase formation observations. The same plots show the loadings at where the two-phase transition first occur. There are no indications that the change of phase influence the VLE. The VLE-data at T=40°C in Figure 3.24 is compared at loading 0.5, which is within the range where two phases are present for systems 3D3M, 3D3.5M and 3.5D3.5M. At this loading the partial pressure of CO_2 is approximately zero for all the systems. Thus, there are no observed differences between the systems which does and does not form two phases in the interval where two phases are present. At loadings above 0.7 the three systems which form two phases has the highest CO_2 partial pressures at T=40°C, and at these loadings all systems are present as one phase.

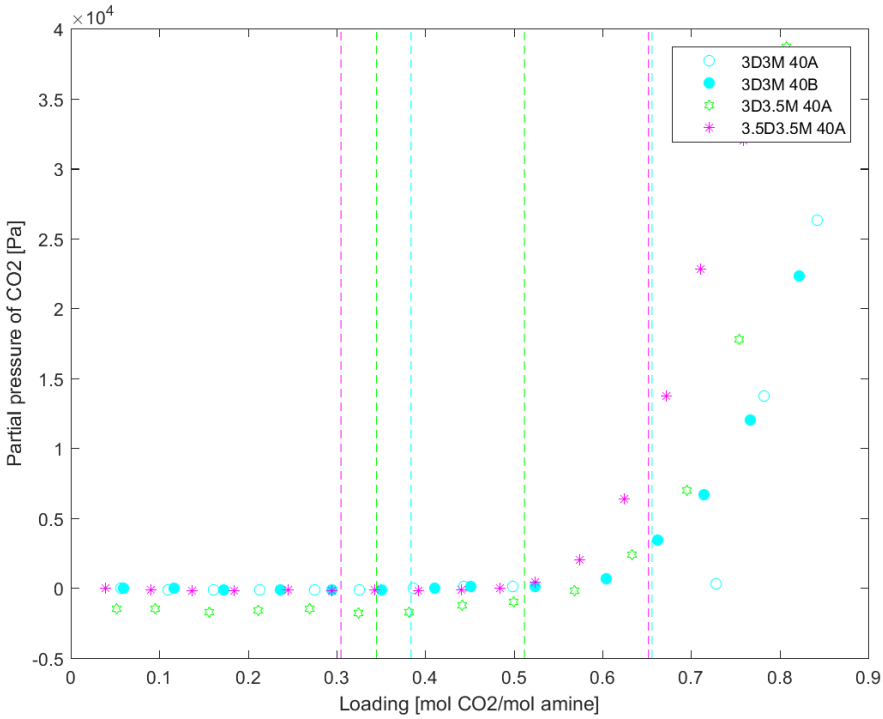

Figure 3.32: VLE-data for systems 3D3M, 3D3.5M and 3.5D3.5M. The vertical lines show the lower and upper limits for the presence of two phases in the system with respective colours.

3.6 Overall performance of solvent systems

(Ciftja et al., 2015) has calculated cyclic capacities based on the loadings where the partial pressure of CO_2 in the systems reach 0.1bar. Rich loadings are the loadings observed at T=40°C and lean loadings at T=80°C. The stripper temperature is normally higher than 80°C, and data from this work at temperature 120°C is further used. If the lean loading in the work by Ciftja was calculated at a higher temperature the lean loading would be lower than numbers reported.

Estimated values for heat of absorption in this work is found at the given lean loading at T=120°C for each system. The partial pressure at T=120°C is found at the same lean loadings. Heat of absorption and CO_2 partial pressure at lean loading are key parameters to determine the performance of the different systems as solvents in a CO_2 capture process. The data for systems investigated in this work is presented in Table 3.4.

Table 3.4: Lean loading, rich loading, Heat of absorption of CO_2 and CO_2 partial pressure. Lean loading and rich loading are from screening experiments by (Ciftja et al., 2015). Heat of absorption and CO_2 partial pressure are values from this work for lean loading at T=120°C.

System	**Rich loading** $[\frac{molCO_2}{molamine}]$	**Lean loading** $[\frac{molCO_2}{molamine}]$	**Heat of absorption** $\frac{kJ}{molCO_2}$	P_{CO_2} [bar]
3D1.5M	0.709	0.418	50	1.15
3D2M	0.656	0.376	90	0.55
1D5M	0.903	0.594	98	0.10
3D3M	0.617	0.354	97	0.20
3D3.5M	0.630	0.363	105	0.25

CO_2 partial pressure at lean loading determines how easily CO_2 is desorbed from the solvent. Of the systems in this work, 3D1.5M has by far the highest partial pressure at lean loading, and 1D5M has the lowest. Of the systems with 3M DEEA the CO_2 partial pressure increases with decreasing concentration of MAPA. Heat of absorption at lean loading in the stripper is another important factor, and determine the energy needed to desorb CO_2 from the solution. A low heat of absorption is desired, as less heat is needed to reverse the absorption reaction. 3D1.5M has the lowest value for heat of absorption of the systems studied, followed by system 3D1.5M. The other systems have both higher heat of absorption and lower CO_2 partial pressures at stripper conditions, and do not appear as good candidates for solvents in a CO_2 absorption process. 3D1.5M is the best choice of the systems studied

here with respect to stripper properties. In this comparison the two-phase formation in systems 3D3M and 3D3.5M is not considered. A phase split followed by stripping of only the phase richest in CO_2 could improve the overall performance of systems with higher MAPA-concentration.

Chapter 4

Conclusions and recommendations

4.1 Conclusions

This work includes experimental studies of two novel alkanolamines for absorption of CO_2 in a CCS-process. These are the tertiary amine 2-(diethylamino)ethanol (DEEA) and the diamine 3-(methylamino)-propylamine (MAPA), with one primary and one secondary amine group. Heat of absorption has been measured in a reaction calorimeter for different blends of the two amines, at the temperatures 40°C, 80°C and 120°C. Most of the blends have been tested twice at each temperature. A total of 5 blends have been studied, whereas 2 of the blends form two liquid phases upon reaction with CO_2. Additionally a sixth blend was tested once at T=40°C, also forming two phases in reaction with CO_2. The same experiments were performed with MEA, which is a well-studied amine and provides a reference for comparison of previous results with results obtained in this work. Samples are collected at the final loading and are analysed by titration. A series of simple experiments are performed on the systems which form two phases, estimating at which loading the two phases first occur.

The results from this work generally correlates well with the results obtained by other researchers for MEA, especially at T=40°C and T=80°C. At T=120°C the deviations are slightly larger, but within an acceptable range. Thus, the results from this work should be considered trustworthy. The degree of deviations between two parallels of the same solution and temperature vary, but is generally within an acceptable range to prove re-

producibility.

The reactor-temperature influences the relative values for heat of absorption within the same solution. Generally, values for heat of absorption in the same solution at loadings up to around 0.3 are lower for T=40°C and highest at T=120°C. The heat of absorption steadily decreases for blends of DEEA-MAPA with increasing loading, unlike pure MAPA-water and DEEA-water systems, which have almost constant values up to a loading around 0.8. Comparing the different blends, the system providing the lowest values for heat of absorption at T=120°C is the 3D1.5M-system. The same system also has the lowest values of heat of absorption at T=40°C up to a loading around 0.4, but at a loading of 1 the system has the *highest* heat of absorption among the systems studied.

Vapour-Liquid-Equilibrium(VLE)-data was obtained from the heat of absorption experiments by assuming constant amine- and water vapour pressure at all CO_2-loadings. The VLE-data correlates well with data obtained by other researchers, supporting the assumption. For the same system at the same loading the CO_2 partial pressure increased with increasing temperature.

Two-phase observations have also been carried out. The heat of absorption experiments are performed in a closed metal reactor, and the exact loading where two phases first occur is not known. The three systems which form two phases have been studied in an open glass cylinder while CO_2 is bubbled through the solution, and the approximate loadings where two phases are present are detected. Assuming the two-phase formation is independent of pressure and temperature, this allow for a discussion weather the two-phase formation impacts the values of heat of absorption and VLE. No drops or increases around the loading of phase transitions are observed in the graphs, thus no clear indications support that the phase change affect the VLE and values for heat of absorption.

The colours of the loaded DEEA/MAPA-systems are observed. There are no clear trends in colour, except from a tendency of decreasing saturation of colours with increasing execution temperature.

There are several sources of error in the experiments which may have affected the final results. The calibration of the reactor calorimeter may have lead to relative differences compared to results obtained by other researchers. The graphical integration of total power, may have caused errors in heat of absorption-values of at least 1.5%. The sampling procedure used in this work has not been satisfactory for use on DEEA/MAPA-systems. The viscosity

of CO_2-loaded DEEA-MAPA is very high, and there were difficulties related to the transfer of loaded sample into the sample cylinder. A second issue is the two-phase formation in many of the systems. There is no way to control how much of each phase that ends up in the sample, and the analysis are not suitable to prove the loading calculated by mass balance.

Based on a discussion around desired properties of a solvent in the stripper section the 3D1.5M blend is the best candidate for a CO_2 absorption process of the systems studied in this work. The solution has the lowest heat of absorption, and the highest partial pressure of CO_2 at stripper conditions.

4.2 Recommendations and future work

The maximum loading capacities of the systems has not been studied in this work. In future experiments the recommendation is to continue the experiments until higher loadings are reached, to obtain a more complete set of data on the heat of absorption. The kinetics of the reactions between the amine-solutions and CO_2 are not considered in this report. In a future study a glass reactor is recommended, to allow for direct observations of two-phase formation at relevant conditions. Further, the sampling procedure needs to be customized to handle sticky solutions, for instance by having a wider pipeline for sampling in the bottom of the reactor. An analysis of loading of each of the phases in a two-phase system would provide useful information for determination of the potential of two-phase systems as solvents in CO_2-capture. For instance, the stirring could be switched off after the last loading to let the system settle for sufficient time, such that sampling of each phase is possible. Such a system would need to have a drain at the top as well as at the bottom. The flowmeter should be properly calibrated prior to the experiments, to validate the amounts of CO_2 added to the reactor calculated by Peng-Robinson equation of state.

Bibliography

Arshad, M., von Solms, N., Thomsen, K., and Svendsen, H. (2013). Heat of absorption of CO2 in aqueous solutions of DEEA, MAPA and their mixture. *Energy Procedia*, 37:1532 – 1542.

Arshad, M. W. (2014). *Measuring and Thermodynamic Modeling of De-Mixing CO2 Capture Systems*. PhD thesis, DTU.

Bernhardsen, I. (November 2015). Conversation about two-phase formation. Ph.D at Norwegian University of Science and Technology (NTNU).

Carey, F. A. and Sundberg, R. J. (2007). *Advanced Organic Chemistry: Part A: Structure and Mechanisms*. Springer Science and Business Media.

CCS (2015). CCS Reg. `http://www.ccsreg.org/technologies.html`. Accessed: 2015-11-26.

ChemiSens (2015). ChemiSens. `http://www.chemisens.se/CMS/`. Accessed: 2015-10-07.

Ciftja, A. F., Hartono, A., Svendsen, H. F., and Knuutila, H. (2015). Two phase formation and cyclic capacity of DEEA-MAPA blends. Poster presentastion at TCCS8 Trondheim, 16-18 june 2015.

CO2crc (2015). CO2 CRC. `http://www.co2crc.com.au/aboutccs/capabsorption.html`. Accessed: 2015-09-07.

Crooks, J. and Donnellan, J. (1990). Kinetics of the Reaction between Carbon Dioxide and Tertary Amines. *J. Org. Chem.*, 55:1372–1374.

Edenhofer, O., Pichs-Madruga, R., Sokona, Y., Farahani, E., Kadner, S., Seyboth, K., Adler, A., Baum, I., Brunner, S., Eickemeier, P., Kriemann, B., Savolainen, J., Schlömer, S., von Stechow, C., Zwickel, T., and (eds.), J. M. (2014). Summary for Policymakers. In: Climate Change 2014: Mitigation of Climate Change. Contribution of Working Group III to the Fifth Assessment Report of the Intergovernmental

Panel on Climate Change. Cambridge University Press, Cambridge, United Kingdom and New York, NY, USA.

Farzad, R. (2014). Modeling of Reaction Calorimeter. Master Thesis: Norwegian University of Science and Technology (NTNU).

Figueroa, J., Fout, T., Plasynski, S., Mcllvried, H., and Srivastava, R. (2008a). Advances in CO2 capture technology - the U.S. Department of Energy's Carbon Sequestration Program. *International Journal of Greenhouse Gas Control*, 2:9–20.

Figueroa, J. D., Fout, T., Plasynski, S., Mcllvried, H., and Srivastava, R. D. (2008b). Advances in CO2 capture technology—The U.S. Department of Energy's Carbon Sequestration Program. *International Journal of Greenhouse Gas Control*, 2:9–20.

Hagewiesche, D., Ashour, S. S., Al-Ghawas, H. A., and Sandall, O. C. (1995). Absorption of Carbon Dioxide into aqueous blends of Monoethanolamine and N-methyldiethanolamine. *Chemical Engineering Science*, 50:1071–1079.

Hartono, A., Saleem, F., Arshad, M. W., Usman, M., and Svendsen, H. F. (2013). Binary and ternary VLE of the 2-(diethylamino)-ethanol (DEEA)/3-(methylamino)-propylamine (MAPA)/water system. *Chemical Engineering Science*, 101:401–411.

IEA (2013). Redrawing the energy-climate map: World energy outlook special report.

Jaubert, J.-N. and Mutelet, F. (2004). VLE predictions with the Peng–Robinson equation of state and temperature dependent kij calculated through a group contribution method. *Fluid Phase Equilibria*, 224:285–304.

Jonassen, ., Kim, I., and F.Svendsen, H. (2014). Heat of absorption of Carbon Dioxide (CO2) into Aqueous N-Methyldiethanolamine (MDEA) and N,N-Dimethylmonoethanolamine (DMMEA). *12th International Conference on Greenhouse Gas Control Technologies, GHGT-12*, 63:1890–1902.

Kanniche, M., Gros-Bonnivard, R., Valle-Marcos, P., Amann, J.-M., and Bouallou, C. (2010). Pre-combustion, post-combustion and oxy-combustion in thermal power plant for CO2 capture. *Applied Thermal Energy*, 30:53–62.

Kim, I. (2009). Heat of reaction and VLE of post combustion CO2 absorb-

ents. Ph.D. thesis, Norwegian University of Science and Technology (NTNU).

Kim, I., Hoff, K. A., and Mejdell, T. (2014). Heat of absorption of CO2 with aqueous solutions of MEA: new experimental data. *Energy Procedia*, 63:1446–1455.

Kim, I. and Svendsen, H. F. (2007a). Heat of Absorption of Carbon Dioxide (CO2) in Monoethanolamine (MEA) and 2-(Aminoethyl)ethanolamine (AEEA) Solutions. *Ind. Eng. Chem. Res.*, 46:5803–5809.

Kim, I. and Svendsen, H. F. (2007b). Heat of Absorption of Carbon dioxide (CO2) in Monoethanolamine (MEA) and 2-(Aminoethyl)ethanolamine (AEEA) solutions. *Ind. Eng. Chem. Res.*, 46:5803–5809.

Kim, S.-T., Kang, J.-W., seop Lee, J., and Min, B.-M. (2011). Analysis of the heat of reaction and regeneration in alkanolamine-CO2 system. *Korean J. Chem. Eng.*, 28(12):2275–2281.

Kim, Y. E., Lim, J. A., Jeong, S. K., Yoon, Y. I., Bae, S. T., and Nam, S. C. (2013). Comparison of Carbon Dioxide Absorption in Aqueous MEA, DEA, TEA, and AMP Solutions. *Bull. Korean Chem. Soc.*, 34:783–787.

Kjelstrup, S. and Helbæk, M. (2006). *Fysikalsk kjemi*. Fagbokforlaget.

Langé, S., Moioli, S., and Pellegrini, L. A. (2015). Vapor-Liquid Equilibrium and Enthalpy of Absorption of the CO2-MEA-H2O System. *Chemical Engineering Transactions*, 43:5803–5809.

Liebenthal, U., Pinto, D., Monteiro, J. G. M.-S., Svendsen, H. F., and Kather, A. (2013). Overall Process Analysis and Optimization for CO2 Capture from Coal Fired Power Plants based in Phase Change Solvents Forming Two Liquid Phases. *Energy Procedia*, 37:1844–1854.

Mathonat, C., Majer, V., Mather, A. E., and Grolier, J.-P. E. (1998). Use of Flow Calorimetry for Determining Enthalpies of Absorption and the Solubility of CO2 in Aqueous Monoethanolamine Solutions. *Ind. Eng. Chem. Res.*, 37:4136–4141.

McCann, N., Maeder, M., and Attalla, M. (2008). Simulation of Enthalpy and Capacity of CO2 absorption by aqueous amine systems. *Ind. Eng. Chem. Res.*, 47:2002–2009.

Monteiro, J. G. M.-S., Majeed, H., Knuutila, H., and Svendsen, H. F. (2015). Kinetics of CO2 absorption in aqueous blends of

N,N-diethylethanolamine (DEEA) and N-methyl-1,3-propane-diamine (MAPA). *Chemical Engineering Science*, 129:145–155.

Pachauri, R. K., Team, I. C. W., and Meyer, L. A. (2014). Climate Change 2014: Synthesis Report. Contribution of Working Groups I, II and III to the Fifth Assessment Report of the Intergovernmental Panel on Climate Change. IPCC, Geneva, Switzerland.

Peng, D.-Y. and Robinson, D. (1976). A New Two-Constant Equation of State. *Ind. Eng. Chem. Fundamen.*, 15(1):59–64.

Pinto, D. (2014). CO2 capture solvents: modeling and experimental characterization.

Pinto, D., amd A. Hartono, S. A. Z., and Svendsen, H. F. (2014a). Evaluation of a phase change solvent for CO2 capture: Absorption and desorption tests. *International Journal of Greenhouse Gas Control*, 28:318–327.

Pinto, D., Monteiro, J. G.-S., Johnsen, B., Svendsen, H. F., and Knuutila, H. (2014b). Density measurements and modelling of loaded and unloaded aqueous solutions of MDEA (N-methyldiethanolamine), DMEA (N,N-diethylethanolamine), DEEA (diethylethanolamine) and MAPA (N-methyl-1,3-diaminepropane). *International Journal of Greenhouse Gas Control*, 25:173–185.

Rennemo, R. (2015b). VLE of Amine Solvents for PCC: Experimental and Modeling: Simplified Report.

Rennemo, R. (November 2015a). Conversation about vle-measurements. Researcher at Norwegian University of Science and Technology (NTNU).

Sartori, G. and Savage, D. W. (1983). Sterically Hindered Amines for CO2 Removal from Gases. *Xnd. Eng. Chem. Fundam.*, 22:239–249.

Schäfer, B., Mather, A., and Marsh, K. (2002). Enthalpies of solution of carbon dioxide in mixed solvents. *Fluid Phase Equilibria*, 194–197:929–935.

Vaidya, P. D. and Kenig, E. Y. (2007). CO2-Alkanolamine Reaction Kinetics: A Review of recent studies. *Chem. Eng. Technol.*, 30:1467–1474.

Vogel, A. I. (1974). *Textbook of Practical Organic Chemistry, 3rd edition.* Longsman.

Yang, H., Xu, Z., Fan, M., Gupta, R., Slimane, R., Bland, A. E., and Wright, I. (2008). Progress in carbon dioxide separaton and capture: A review. *Environmental Sciences*, 20:14–27.

Yu, K. M. K., Curcic, I., Gabriel, J., and Tsang, S. C. E. (2008). Recent Advances in CO2 Capture and Utilization. *Chem.Sus.Chem.*, 1.

Appendix A

Calibration

The results from the calibration sequence, yielding a series of FlowCP-values for the temperatures 40, 80 and 120 $°C$, are presented in Table A.1. The table also includes the FlowCP-value which is decided used in the heat of absorption-experiments at each of the temperatures.

Table A.1: Estimated FlowCP-values from calibration sequences at temperatures 40, 80 and 120$°C$

Experiment	**FlowCP 40**$°C$	**FlowCP 80**$°C$	**FlowCP 120**$°C$
Exp. A	420	460	472
Exp. B	420	462	472
	419	462	474
			480
Used FlowCP	420	462	475

Appendix B

Results

B.1 30 wt% MEA

Table B.1: 30 wt% MEA

40°C- A	
Loading [mol/mol]	Heat [kJ/mol CO_2]
0.045	87.514
0.122	83.896
0.152	82.633
0.204	81.697
0.254	86.620
0.304	87.007
0.353	87.711
0.401	86.413
0.449	79.552
0.493	61.561
0.582	44.261

80°C- A	
Loading [mol/mol]	Heat [kJ/mol]
0.035	107.146
0.079	90.411
0.123	89.111
0.170	89.045
0.212	89.222
0.256	88.356
0.301	92.429
0.349	85.767
0.396	85.574
0.444	83.677
0.491	74.449
0.539	54.010

120°C- A		**80°C- B**	
Loading [mol/mol]	Heat [kJ/mol CO_2]	Loading [mol/mol]	Heat [kJ/mol]
0.045	139.421	0.055	93.196
0.091	97.577	0.120	90.844
0.139	98.727	0.171	89.916
0.187	93.465	0.223	90.570
0.228	95.006	0.273	88.600
0.274	92.709	0.337	88.592
0.316	88.786	0.392	85.628
0.359	88.349	0.438	80.446
0.397	86.679	0.493	68.038
0.438	57.844	0.523	40.577

B.2 Heat of absorption measurements

B.2.1 3M DEEA + 1.5M MAPA

Table B.3: 3D1.5M 40

40°C- A	
Loading [mol/mol]	Heat [kJ/mol CO_2]
0.071	90.776
0.157	89.560
0.233	88.624
0.284	90.479
0.333	91.654
0.413	87.662
0.500	88.177
0.580	89.170
0.661	90.746
0.744	90.314
0.829	88.151
0.916	79.852
1.033	52.070

40°C- B	
Loading [mol/mol]	Heat [kJ/mol]
0.081	88.713
0.157	90.569
0.249	88.894
0.327	89.228
0.406	88.467
0.486	88.791
0.566	91.246
0.646	90.090
0.731	90.170

Table B.4: 3M DEEA + 1.5M MAPA at 80 °C

80°C- A	
Loading [mol/mol]	Heat [kJ/mol]
0.056	115.543
0.110	115.773
0.160	109.174
0.242	104.623
0.290	105.491
0.349	98.628
0.447	84.371
0.485	100.386
0.522	97.295
0.559	89.342
0.602	71.592

80°C- B	
Loading [mol/mol]	Heat [kJ/mol]
0.081	96.013
0.173	94.724
0.248	92.872
0.310	90.863
0.384	94.739
0.449	91.408
0.525	90.917
0.605	91.432
0.686	89.758
0.761	88.480
0.841	85.147
0.926	72.081

Table B.5: 3M DEEA + 1.5M MAPA at 120 °C

120°C- A	
Loading [mol/mol]	Heat [kJ/mol]
0.048	95.837
0.107	108.719
0.172	100.139
0.236	92.981
0.306	89.736
0.363	84.285
0.426	56.565

Table B.6: 3D2M 40

40°C- A	
Loading [mol/mol]	Heat [kJ/mol CO_2]
0.050	96.025
0.102	93.613
0.157	94.050
0.206	89.684
0.257	91.400
0.306	91.232
0.353	88.237
0.400	85.476
0.449	84.746
0.496	81.029
0.547	76.801
0.604	71.547
0.656	68.910
0.715	66.748
0.780	60.867
0.866	54.351

40°C- B	
Loading [mol/mol]	Heat [kJ/mol]
0.077	96.568
0.152	93.592
0.223	93.704
0.299	90.116
0.386	87.758
0.456	82.949
0.528	78.275
0.627	72.023
0.705	65.487
0.778	60.845

B.2.2 3M DEEA + 2M MAPA

Table B.7: 3M DEEA + 2M MAPA at 80 °C

80°C- A	
Loading [mol/mol]	Heat [kJ/mol]
0.060	101.343
0.113	99.945
0.171	97.909
0.226	94.587
0.278	92.562
0.332	90.078
0.392	88.866
0.446	83.491
0.505	79.328
0.561	76.101
0.612	72.351
0.665	74.161
0.706	59.841

80°C- B	
Loading [mol/mol]	Heat [kJ/mol]
0.069	100.348
0.120	99.933
0.200	97.444
0.269	93.830
0.338	89.745
0.405	87.626
0.481	80.994
0.548	77.839
0.626	67.966

Table B.8: 3M DEEA + 2M MAPA at 120 °C

120°C- A	
Loading [mol/mol]	Heat [kJ/mol]
0.055	51.397
0.112	112.978
0.170	100.511
0.227	99.001
0.283	95.719
0.337	90.776
0.394	83.622
0.445	61.722

120°C- B	
Loading [mol/mol]	Heat [kJ/mol]
0.066	107.554
0.133	107.092
0.196	100.023
0.270	98.751
0.332	95.219
0.377	88.317
0.419	78.394

B.2.3 1M DEEA + 5M MAPA

Table B.9: 1M DEEA +5M MAPA at 40 °C

40°C- A	
Loading [mol/mol]	Heat [kJ/mol CO_2]
0.050	105.874
0.096	99.937
0.144	99.583
0.197	100.371
0.250	100.901
0.303	100.279
0.357	97.795
0.409	98.135
0.466	95.735
0.518	96.688
0.578	95.200
0.640	94.198
0.705	91.255
0.772	89.831
0.835	85.494
0.891	73.545
0.923	60.956

40°C- B	
Loading [mol/mol]	Heat [kJ/mol]
0.065	105.719
0.133	99.898
0.194	103.162
0.261	99.108
0.332	100.259
0.384	99.703
0.447	97.073
0.520	96.694
0.594	94.769
0.660	93.177
0.729	93.097
0.802	88.342
0.877	76.120
0.939	57.749

Table B.10: 1M DEEA + 5M MAPA at 80 °C

80°C- A	
Loading [mol/mol]	Heat [kJ/mol]
0.067	107.317
0.121	107.819
0.176	106.075
0.236	105.926
0.296	104.417
0.354	104.864
0.448	103.207
0.500	102.758
0.559	100.150
0.610	99.815
0.676	97.528
0.736	93.701
0.798	88.367
0.847	81.715

80°C- B	
Loading [mol/mol]	Heat [kJ/mol]
0.062	106.885
0.132	105.301
0.212	105.580
0.271	102.690
0.332	102.933
0.389	102.045
0.449	101.966
0.510	100.013
0.571	97.940
0.639	93.452
0.723	92.526
0.788	87.805
0.851	81.140
0.902	70.137

Table B.11: 1M DEEA + 5M MAPA at 120 °C

120°C- A	
Loading [mol/mol]	Heat [kJ/mol]
0.061	109.445
0.109	108.058
0.168	105.824
0.258	105.859
0.297	102.805
0.337	103.245
0.388	102.692
0.442	100.317
0.508	100.951
0.576	96.679

120°C- B	
Loading [mol/mol]	Heat [kJ/mol]
0.060	109.960
0.111	106.630
0.165	105.899
0.220	105.295
0.273	84.973
0.329	104.078
0.386	100.847
0.438	101.299
0.492	99.086
0.546	100.647
0.609	96.289

B.2.4 3M DEEA +3M MAPA

Table B.12: 3M DEEA +3M MAPA at 40 °C

40°C- A	
Loading [mol/mol]	Heat [kJ/mol CO_2]
0.056	98.928
0.110	99.248
0.162	97.741
0.213	96.152
0.275	94.726
0.326	93.089
0.386	91.695
0.443	90.752
0.499	88.645
0.728	76.128
0.783	62.101
0.843	57.553

40°C- B	
Loading [mol/mol]	Heat [kJ/mol]
0.060	101.764
0.116	99.475
0.172	98.974
0.237	95.685
0.295	96.086
0.351	93.203
0.411	91.682
0.451	90.560
0.524	86.405
0.605	79.507
0.662	74.657
0.715	70.765
0.767	63.510
0.822	60.328

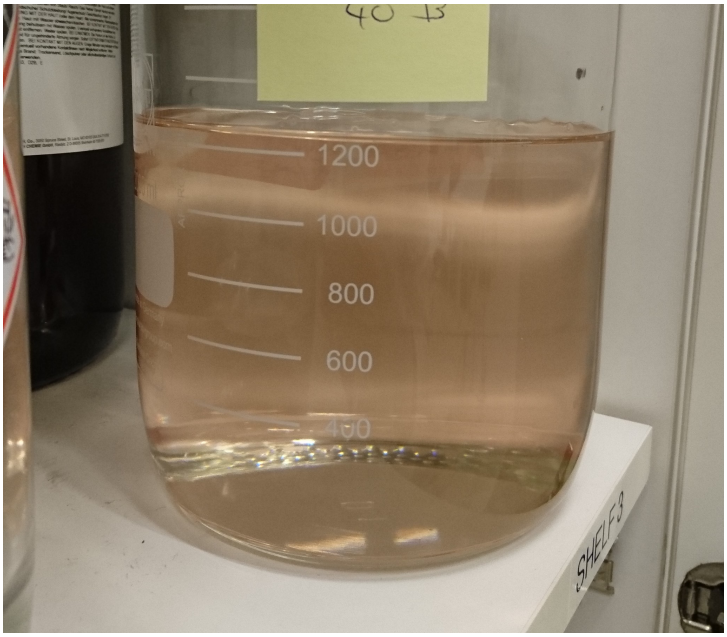

Figure B.1: Picture of loaded solution, experiment 3D3M-40-A

Table B.13: 3M DEEA + 3M MAPA at 80 °C

80°C- A	
Loading [mol/mol]	Heat [kJ/mol]
0.058	104.366
0.114	102.733
0.169	101.475
0.226	100.229
0.282	96.407
0.338	96.272
0.397	95.153
0.452	91.808
0.507	86.172
0.562	79.192
0.617	74.898

80°C- B	
Loading [mol/mol]	Heat [kJ/mol]
0.055	107.866
0.116	104.119
0.174	102.707
0.230	101.001
0.303	100.302
0.370	95.619
0.431	92.262
0.488	88.214
0.547	79.906
0.602	75.732

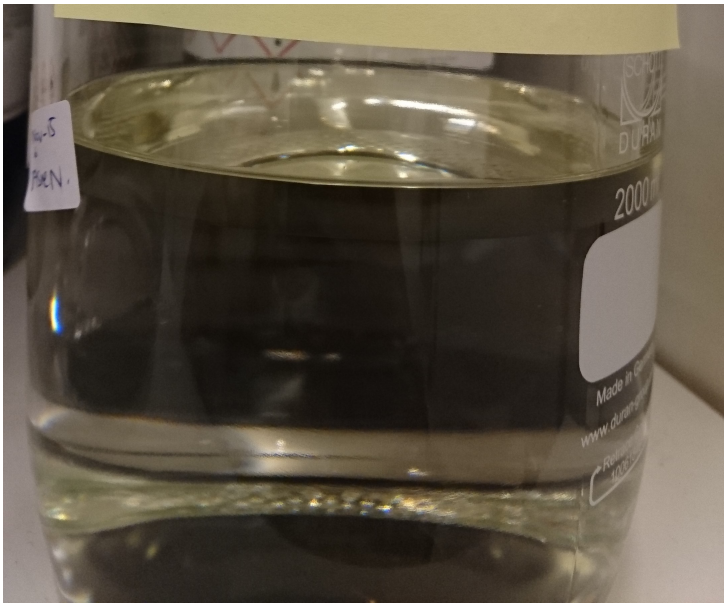

Figure B.2: Picture of loaded solution, 3D3M-80A

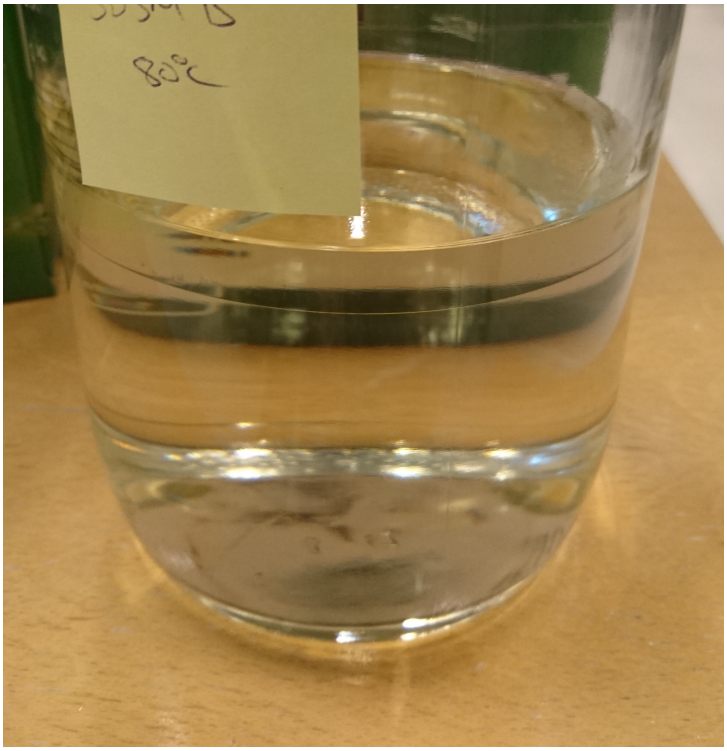

Figure B.3: Picture of loaded solution, 3D3M-80B

Table B.14: 3M DEEA + 3M MAPA at 120 °C

120°C- A	
Loading [mol/mol]	Heat [kJ/mol]
0.054	106.633
0.104	115.797
0.225	105.439
0.266	100.328
0.312	98.190
0.356	97.116
0.413	92.735
0.463	86.683

120°C- B	
Loading [mol/mol]	Heat [kJ/mol]
0.061	105.360
0.112	111.595
0.167	104.905
0.214	102.197
0.254	103.329
0.292	99.676
0.352	96.555
0.403	93.561
0.446	88.935
0.485	76.557

Figure B.4: Picture of loaded solution, 3D3M-120A

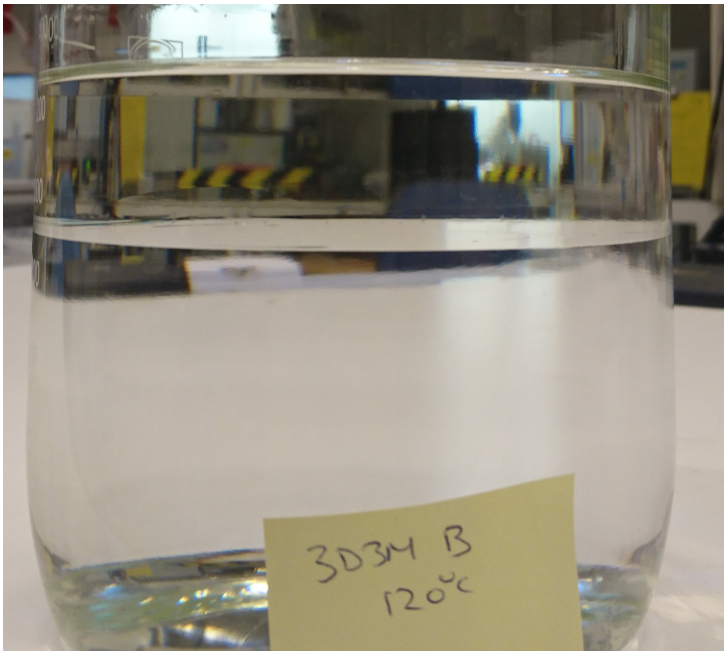

Figure B.5: Picture of loaded solution, 3D3M-120B

B.2.5 3M DEEA + 3.5M MAPA

Table B.15: 3M DEEA + 3.5M MAPA at 40 °C

40°C- A	
Loading [mol/mol]	Heat [kJ/mol]
0.052	110.257
0.096	106.110
0.157	105.513
0.212	106.318
0.269	101.415
0.324	105.000
0.382	99.406
0.441	99.786
0.500	97.054
0.568	87.946
0.633	82.344
0.696	74.762
0.755	83.603
0.808	61.974

40°C- B	
Loading [mol/mol]	Heat [kJ/mol]
0.065	107.143
0.121	107.396
0.177	107.030
0.248	104.423
0.311	103.336
0.338	103.026
0.410	101.908
0.487	97.877
0.547	89.812
0.607	84.108
0.654	80.832
0.720	76.107
0.780	70.548

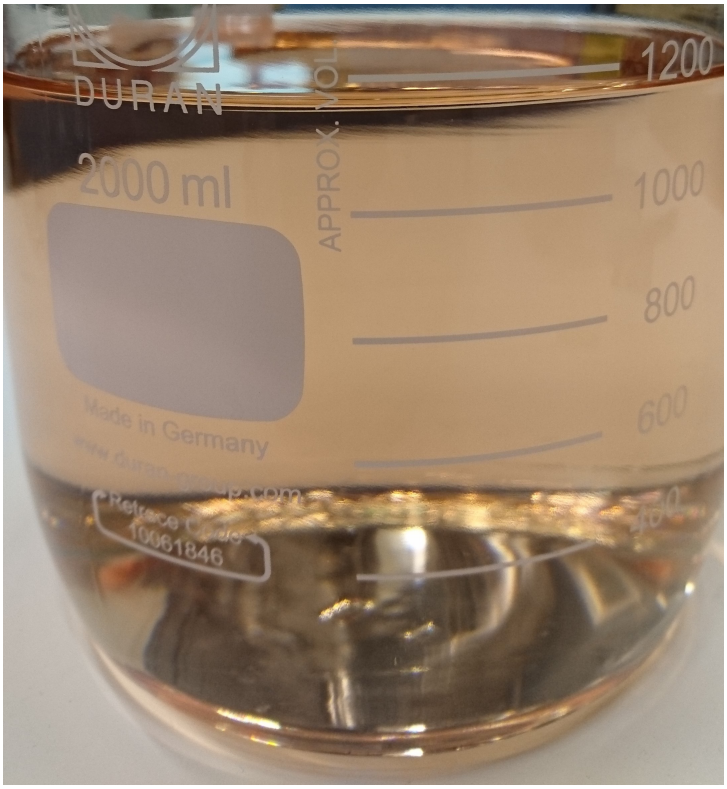

Figure B.6: Picture of loaded solution, 3D3.5M-40B

Table B.16: 3M DEEA + 3.5M MAPA at 80 °C

80°C- A	
Loading [mol/mol]	Heat [kJ/mol]
0.064	108.993
0.103	106.482
0.162	105.224
0.218	106.534
0.271	102.955
0.329	99.312
0.398	98.976
0.453	93.998
0.513	90.081
0.567	83.168
0.624	75.976
0.678	71.327
0.714	68.849

80°C- B	
Loading [mol/mol]	Heat [kJ/mol]
0.036	108.355
0.105	109.308
0.164	107.905
0.230	101.721
0.289	105.382
0.356	101.956
0.417	99.770
0.474	99.449
0.535	88.680
0.594	76.665
0.652	70.788

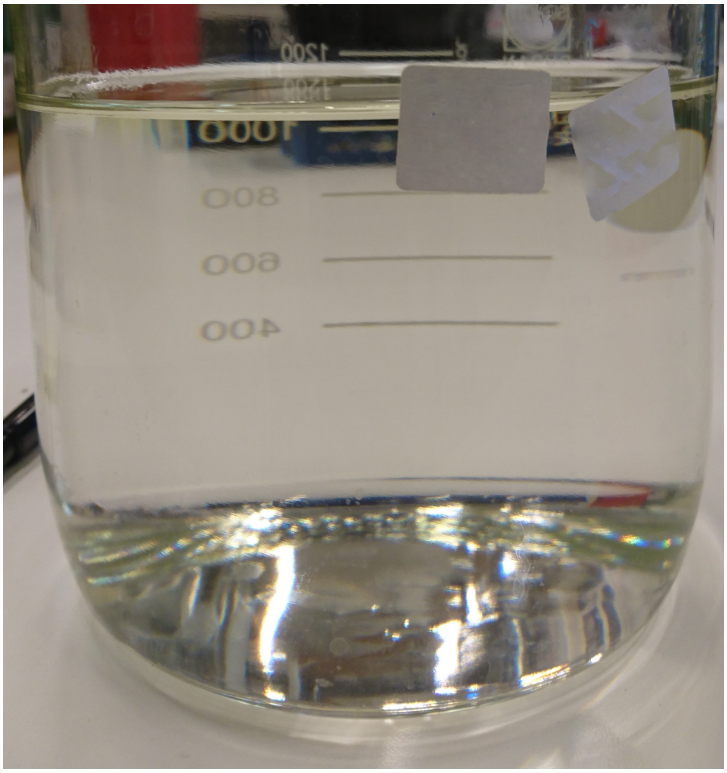

Figure B.7: Picture of loaded solution, 3D3.5M-80A

Table B.17: 3M DEEA + 3.5M MAPA at 120 °C

120°C- A	
Loading [mol/mol]	Heat [kJ/mol]
0.054	111.928
0.108	108.677
0.149	106.370
0.201	104.315
0.307	103.593
0.358	100.924
0.379	95.362
0.414	96.220
0.449	92.560
0.471	90.419
0.508	62.473

120°C- B	
Loading [mol/mol]	Heat [kJ/mol]
0.051	134.139
0.102	108.117
0.155	110.523
0.213	109.829
0.270	107.868
0.319	109.497
0.389	103.489
0.439	96.643
0.487	92.325
0.517	53.830

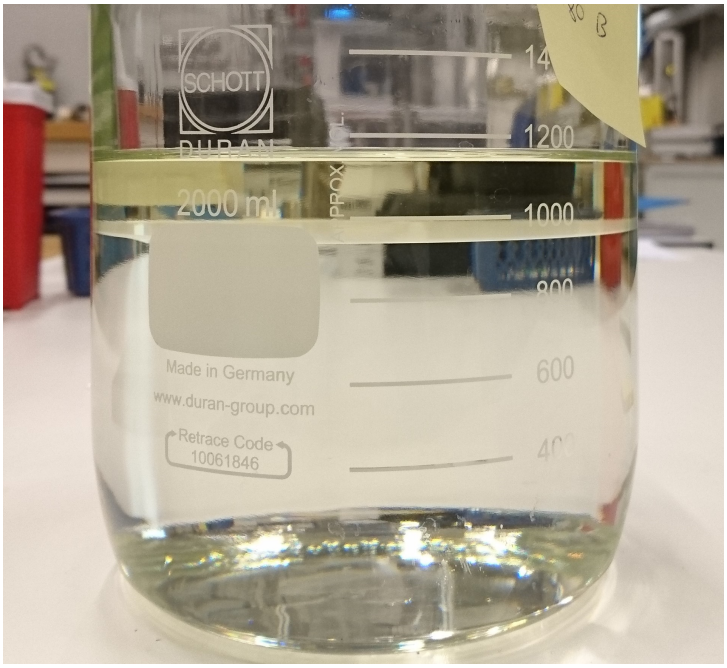

Figure B.8: Picture of loaded solution, 3D3.5M-80A

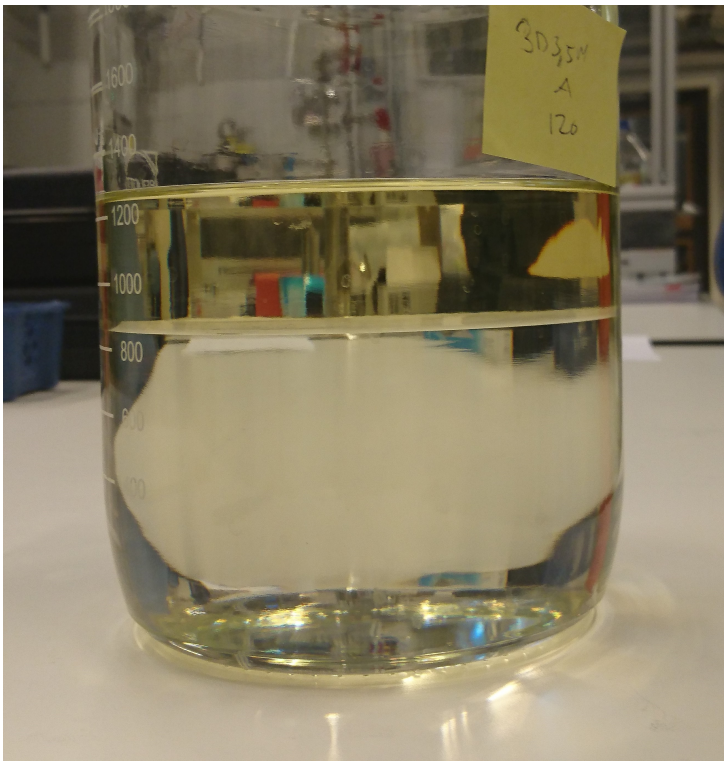

Figure B.9: Picture of loaded solution, 3D3.5M-120A

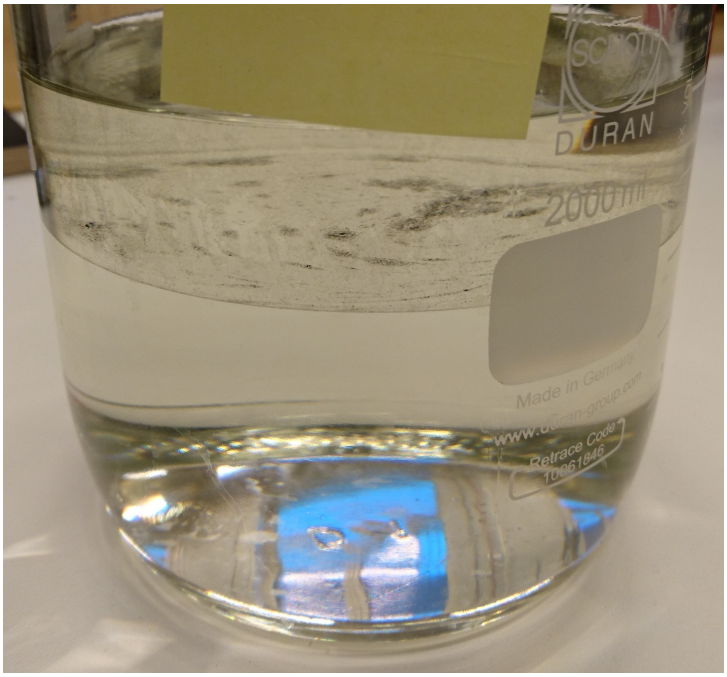

Figure B.10: Picture of loaded solution, 3D3.5M-120B

B.2.6 3.5M DEEA + 3.5M MAPA

Table B.18: 3.5M DEEA +3.5M MAPA at 40 °C

40°C- A	
Loading [mol/mol]	Heat [kJ/mol CO_2]
0.039	105.580
0.091	105.469
0.137	104.013
0.185	101.386
0.245	100.166
0.295	97.130
0.343	96.317
0.393	95.466
0.441	95.045
0.485	87.467
0.524	83.897
0.574	78.679
0.624	74.504
0.672	75.857
0.711	72.092
0.759	69.023

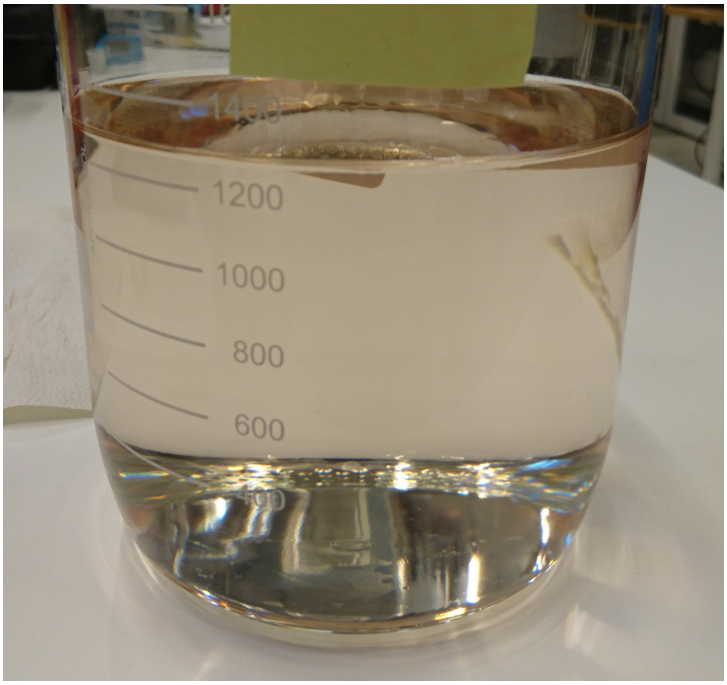

Figure B.11: Picture of the loaded solution of experiment 3.5D3.5M-40-A.

B.3 VLE

VLE-data from experiments performed at the same temperature are plotted in the same figures in Figure B.12-Figure B.14, as a function of loading calculated per number of amine groups.

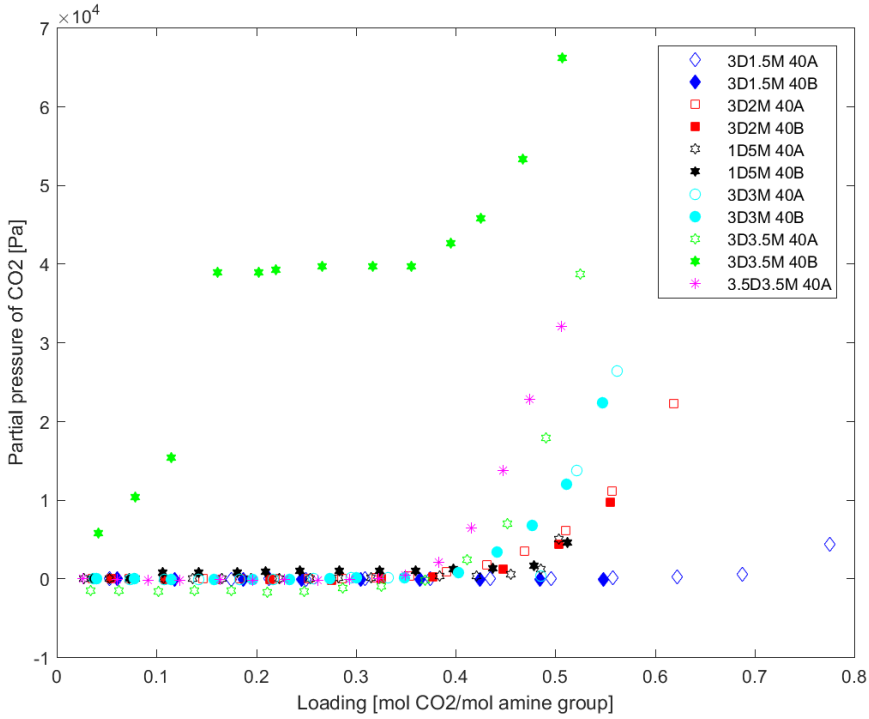

Figure B.12: CO_2 partial pressure plotted as a function of loading, where the loading is found as mole CO_2 per moles of amine *groups*. Here at T=40°C

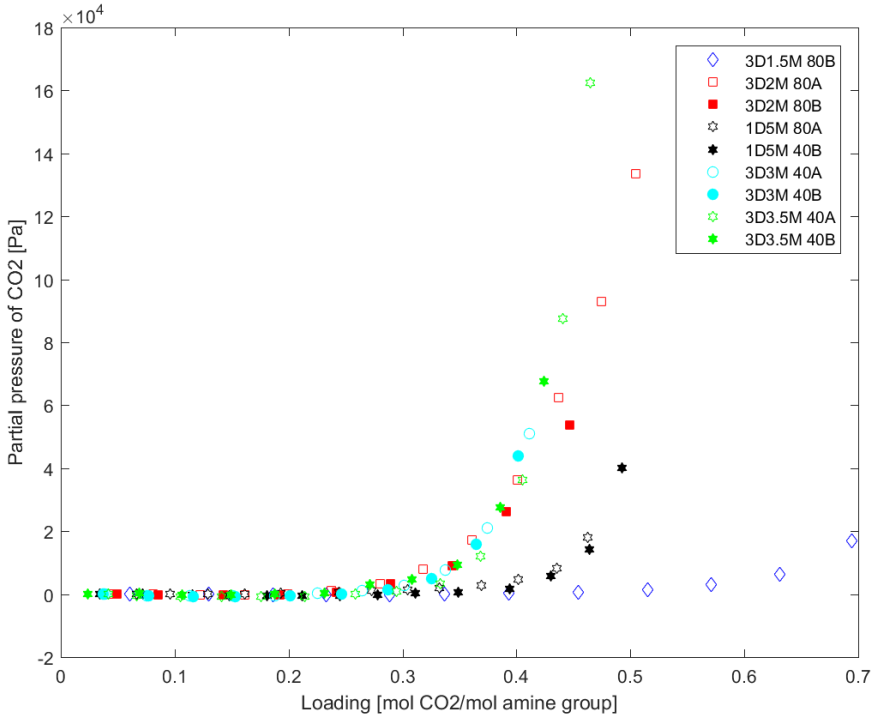

Figure B.13: CO_2 partial pressure plotted as a function of loading, where the loading is found as mole CO_2 per moles of amine *groups*. Here at T=80°C.

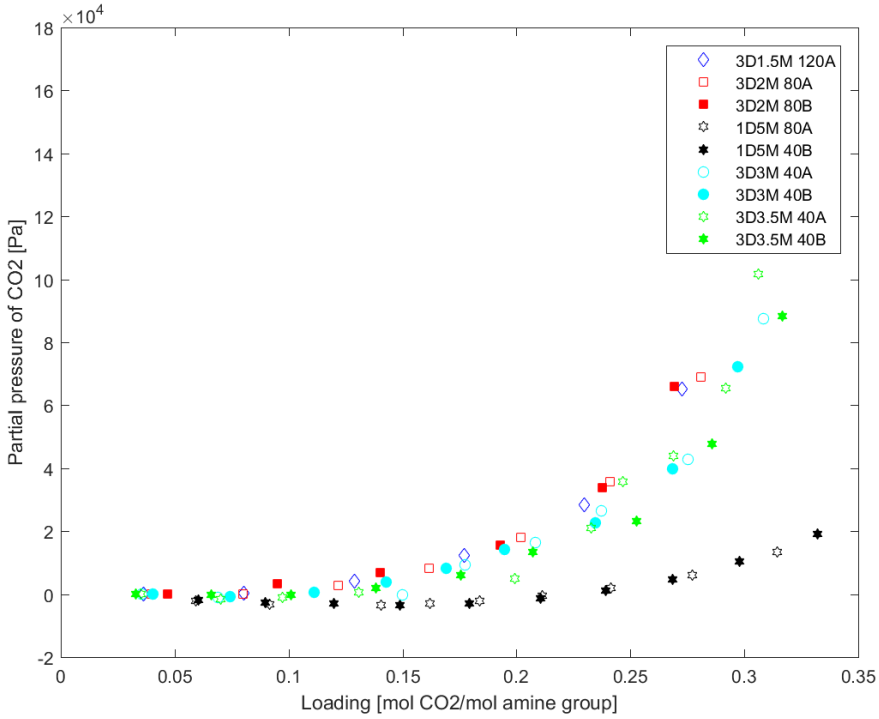

Figure B.14: CO_2 partial pressure plotted as a function of loading, where the loading is found as mole CO_2 per moles of amine *groups*. Here at T=120°C.

Appendix C

MSDSs

The following sides include Material Safety Data Sheets for the amines used in this work.

SAFETY DATA SHEET

according to Regulation (EC) No. 453/2010
Version 6.0 Revision Date 16.07.2015
Print Date 28.09.2015
GENERIC EU MSDS - NO COUNTRY SPECIFIC DATA - NO OEL DATA

SECTION 1: Identification of the substance/mixture and of the company/undertaking

1.1 Product identifiers

Product name	:	Ethanolamine
Product Number	:	398136
Brand	:	Sigma-Aldrich
Index-No.	:	603-030-00-8
REACH No.	:	A registration number is not available for this substance as the substance or its uses are exempted from registration, the annual tonnage does not require a registration or the registration is envisaged for a later registration deadline.
CAS-No.	:	141-43-5

1.2 Relevant identified uses of the substance or mixture and uses advised against

Identified uses	:	Laboratory chemicals, Manufacture of substances

1.3 Details of the supplier of the safety data sheet

Company	:	Sigma-Aldrich Norway AS Filipstad Brygge 1 N-0252 OSLO
Telephone	:	+47 23 176000
Fax	:	+47 23 176010
E-mail address	:	eurtechserv@sial.com

1.4 Emergency telephone number

Emergency Phone #	Giftinformasjonssentralen 22 59 13 00

SECTION 2: Hazards identification

2.1 Classification of the substance or mixture

Classification according to Regulation (EC) No 1272/2008

Acute toxicity, Oral (Category 4), H302
Acute toxicity, Inhalation (Category 4), H332
Acute toxicity, Dermal (Category 4), H312
Skin corrosion (Category 1B), H314
Chronic aquatic toxicity (Category 3), H412
Specific target organ toxicity - single exposure (Category 3), Respiratory system, H335

For the full text of the H-Statements mentioned in this Section, see Section 16.

2.2 Label elements

Labelling according Regulation (EC) No 1272/2008

Pictogram

Signal word Danger

SAFETY DATA SHEET

according to Regulation (EC) No. 1907/2006
Version 5.0 Revision Date 20.12.2012
Print Date 28.09.2015
GENERIC EU MSDS - NO COUNTRY SPECIFIC DATA - NO OEL DATA

1. IDENTIFICATION OF THE SUBSTANCE/MIXTURE AND OF THE COMPANY/UNDERTAKING

1.1 Product identifiers

Product name	:	2-(Diethylamino)ethanol
Product Number	:	471321
Brand	:	Aldrich
Index-No.	:	603-048-00-6
CAS-No.	:	100-37-8

1.2 Relevant identified uses of the substance or mixture and uses advised against

Identified uses	:	Laboratory chemicals, Manufacture of substances

1.3 Details of the supplier of the safety data sheet

Company	:	Sigma-Aldrich Norway AS Filipstad Brygge 1 N-0252 OSLO
Telephone	:	+47 23 176000
Fax	:	+47 23 176010
E-mail address	:	eurtechserv@sial.com

1.4 Emergency telephone number

Emergency Phone #	:	Giftinformasjonssentralen 22 59 13 00

2. HAZARDS IDENTIFICATION

2.1 Classification of the substance or mixture

Classification according to Regulation (EC) No 1272/2008 [EU-GHS/CLP]
Flammable liquids (Category 3)
Acute toxicity, Oral (Category 4)
Acute toxicity, Inhalation (Category 4)
Acute toxicity, Dermal (Category 4)
Skin corrosion (Category 1B)
Skin sensitization (Category 1)

Classification according to EU Directives 67/548/EEC or 1999/45/EC
Causes burns. Flammable. Harmful by inhalation, in contact with skin and if swallowed.

2.2 Label elements

Labelling according Regulation (EC) No 1272/2008 [CLP]
Pictogram

Signal word Danger

Hazard statement(s)

H226	Flammable liquid and vapour.
H302	Harmful if swallowed.
H312	Harmful in contact with skin.
H314	Causes severe skin burns and eye damage.
H317	May cause an allergic skin reaction.
H332	Harmful if inhaled.

SAFETY DATA SHEET

according to Regulation (EC) No. 1907/2006
Version 5.4 Revision Date 18.06.2015
Print Date 28.09.2015
GENERIC EU MSDS - NO COUNTRY SPECIFIC DATA - NO OEL DATA

SECTION 1: Identification of the substance/mixture and of the company/undertaking

1.1 Product identifiers

Product name	:	3-(Methylamino)propylamine
Product Number	:	65690
Brand	:	Sigma-Aldrich
REACH No.	:	A registration number is not available for this substance as the substance or its uses are exempted from registration, the annual tonnage does not require a registration or the registration is envisaged for a later registration deadline.
CAS-No.	:	6291-84-5

1.2 Relevant identified uses of the substance or mixture and uses advised against

Identified uses	:	Laboratory chemicals, Manufacture of substances

1.3 Details of the supplier of the safety data sheet

Company	:	Sigma-Aldrich Norway AS Filipstad Brygge 1 N-0252 OSLO
Telephone	:	+47 23 176000
Fax	:	+47 23 176010
E-mail address	:	eurtechserv@sial.com

1.4 Emergency telephone number

Emergency Phone # Giftinformasjonssentralen 22 59 13 00

SECTION 2: Hazards identification

2.1 Classification of the substance or mixture

Classification according to Regulation (EC) No 1272/2008
Flammable liquids (Category 3), H226
Acute toxicity, Inhalation (Category 1), H330
Acute toxicity, Dermal (Category 4), H312
Acute toxicity, Oral (Category 4), H302
Skin corrosion (Category 1B), H314

For the full text of the H-Statements mentioned in this Section, see Section 16.

Classification according to EU Directives 67/548/EEC or 1999/45/EC
F, C Highly flammable, Corrosive R10, R20/21/22, R34

For the full text of the R-phrases mentioned in this Section, see Section 16.

2.2 Label elements

Labelling according Regulation (EC) No 1272/2008
Pictogram

Signal word Danger